Spectral Occupancy Analysis of VLA RFI Survey Observations (2013–2026)

Frank K. Schinzel[1] and Aaron Lawson[1]
[1]Spectrum Management Department (SMD)

Date: August 13, 2026
Keys: VLA, band studies
Internal Reference Tag: None

Abstract

An analysis of spectral occupancy at the Karl G. Jansky Very Large Array (VLA) is presented, based on dedicated RFI survey observations conducted between 2013 and 2026, covering the P-band receiver (224—480 MHz) and the L- through Q-band receivers (1—50 GHz). Occupancy was determined per receiver band, per 128 MHz spectral window (16 MHz for P-band), and for custom frequency ranges of interest, using vector-averaged cross-correlations from fixed, shortest, and longest baseline sets with an empirically determined noise threshold. Over the past decade, spectral occupancy has increased at rates of 0.77±0.11%/year at L-band, 0.19±0.15%/ year at S-band, and 0.422±0.062%/year at C-band, corresponding to a cumulative loss in usable bandwidth of roughly 145 MHz, 152 MHz, and 244 MHz respectively, with an additional 204 MHz lost at X-band. Frequencies above 18 GHz remain virtually unoccupied. Southern pointings, added in 2024, show systematically higher occupancy than the Northern Celestial Pole pointing in most bands. Additional analysis covers bands under NTIA study for potential commercial wireless use, ISM/WiFi bands, IMT bands, GNSS allocations, select satellite bands, and ITU-protected radio astronomy bands. Notable recent developments include new IMT transmissions from a nearby cell tower upgrade affecting L and S bands, locally generated 5.8 GHz interference from motion-detecting light bulbs that was subsequently mitigated, and the near-total occupancy of the 1 990—1 995 MHz range by Starlink Direct-to-Device (D2D) service. These results document the continuing erosion of usable spectrum for radio astronomy at the VLA, driven primarily by satellite constellations, terrestrial wireless expansion, and local emissions.

Contents

Changelog

2026.08.13.0 Frank K. Schinzel et al. — Initial published version.

1 Background

With the completion of the Expanded VLA (EVLA) project, the VLA has been performing regular observations to monitor the RFI environment since 2011. These observations are done using all receivers from L-band to Q-band (1–50 GHz), along with the P-band receiver (224–480 MHz) which was added in 2016. The observing cadence was originally a single observation per VLA configuration, however, since the 2024 B-configuration this cadence has quickened to once every two weeks.

All observations before the 2024 B-configuration were done by looking at the North Celestial Pole (NCP). Observing the NCP was chosen in an attempt to maximize RFI signal correlation by minimizing attenuation due to fringe winding, an effect described in Perley (2002). In an attempt to better monitor the RFI environment, starting with the 2024 A-configuration observations began including a pointing towards the south ($\sim$34° elevation, $\sim$180° azimuth). In the southern observations the fringe winding is approximately removed via software to minimize signal de-correlation.

All observations until mid 2025 used a channel width of 125 kHz. Due to an unresolved hardware issue within the WIDAR correlator,[1] all observations afterwards have been done using a channel width of 143 kHz. Regardless of channel width or pointing direction all observations haven been conducted using the 8-bit samplers. All historic data is available in its raw format via the NRAO's data archive and array averaged plots are available via NRAO's Dynamic Radio Interference Finding Tool (DRIFT)[2].

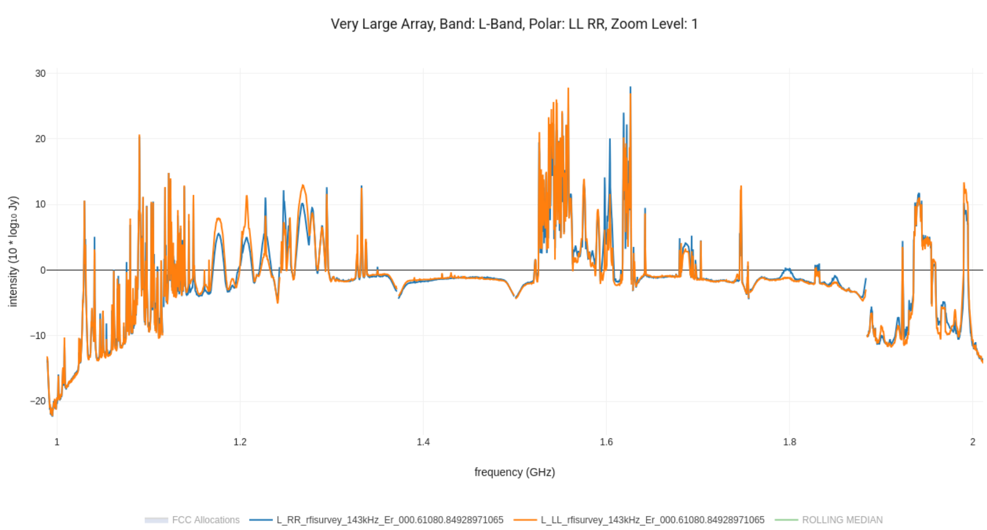

Figure 1: Example spectra of VLA L-Band RFI Sweep data visualized with DRIFT. Note: Unlike the data processing described in Section 2, the data processing of the DRIFT data includes calibration via the antenna system temperature measurements and is scalar averaged across all baselines.

2 Data Processing

This analysis used 93 VLA RFI Scans that were deemed usable for the here presented analysis: 54x 125 kHz NCP observations, 7x 125 kHz southern observations, 15x 143 kHz NCP observations, and 17x 143 kHz southern observations. From each of these observations the vector averaged data was obtained using a combination of baselines: 1) the three furthest antennas in each arm of the array;

[1] https://science.nrao.edu/facilities/vla/docs/manuals/oss2026b/widar
[2] drift.nrao.edu

hb!

Table 1: Noise threshold multiplication factors for each VLA receiver that were empirically determined.

Receiver	Factor
P	5
L	3
S	5
C	5
X	6
Ku	5
K	5
Ka	10
Q	6

2) the three central most antennas in each arm of the array; 3) the antennas on the eighth pad of each arm in the array, 4) and the combination of all baselines available. Note that the VLA is reconfigurable and the antenna locations/baselines are changing on a ∼4 month time scale with the configuration changes. Only the eighth pad of each arm is guaranteed to have an active antenna. This allowed for data collection from the longest baselines, the shortest baselines, and fixed/unchanging baselines. For each observation, the data was loaded into CASA and then the averages were computed using numpy for each set of nominally three baselines. The only other processing of note was the application of Hanning smoothing to remove ringing effects related to the Gibbs phenomenon. The processed data were then loaded into `HDF5` files together with corresponding metadata for further processing. From these files additional processing determined spectral occupancies per receiver and spectral windows, as well as custom defined frequency ranges of interest and were imported into a SQLite database for ease of access.

3 Spectral Occupancy Determination

Spectral occupancy was determined for each receiver band, 128 MHz spectral windows, and custom frequency ranges using the fully pre-averaged and fully channelized data provided in the `HDF5` files. In the case of the P-band receiver (224–480 MHz) the two linearly polarized signals were recorded, while for all the other receivers two circular polarizations are recorded. To simplify data processing, the two polarization correlation products, either XX&YY or RR&LL, are combined to form what is considered a total intensity $\frac{(\mathrm{XX/RR+YY/LL})}{2}$. In the first step, the noise floor of the data was approximated for each spectrum from the different combination of baselines. To do so, the channelized unflagged data[3] for each receiver band is sorted from the largest to the smallest values. Then the bottom 75% of values are used to calculate mean and rms values. The sum of both is used to clip the highest values from the dataset to reduce the number of high value outliers. After this, the median from the remaining values is determined and used as noise floor threshold. In the next step, this threshold is used to determine whether a channel value lies above or below this threshold multiplied by an empirically determined adjustment factor that depends on the receiver band. These factors are listed in Table 1 for reference. Across the date range analyzed this approach captured a consistent threshold from dataset to dataset.

The approach taken for determination of the noise threshold does not follow common methods where the bottom 20% of data is typically used and then scaled up by a factor of 3 or 6 dB. The spectral response of the receiver, baseband filter, and finite response spectral window filters complicate determination of a true noise floor. Figure 2 shows an example spectrum for the VLA C-band and NCP pointing both scalar and vector averaged cross-correlations for the three 8-pad antenna baselines. It is immediately apparent that the vector averaged data shows a weaker correlation of the spectral window

[3] only the inner 60% of channels are used of each 128 MHz spectral window.

filter shapes and therefore it was decided to use that approach that the risk of losing some incoherent signals due to the type of averaging, while allowing for better determination of the noise threshold.

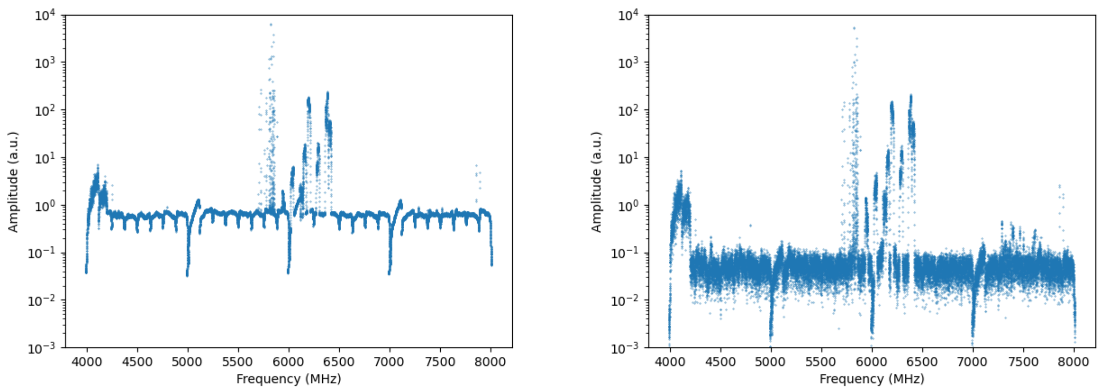

Figure 2: *Left:* Scalar averaged cross-correlation spectrum of fixed 8-pad VLA antenna for dataset `rfisurvey_125kHz.60519.956562824074` (2024-07-28) with the VLA in B configuration. *Right:* Similarly the vector averaged spectrum of fixed pad antenna cross-correlations.

The spectral occupancy for a set bandwidth was then determined taking all spectral channels (typically of 1 MHz width each) and determining the fraction that lied above and below the corresponding threshold adjusted by the above discussed multiplication factor. In addition, the average factor above the threshold as well as the maximum factor above the threshold for any of the evaluated channels was recorded. Another more realistic occupancy factor was determined that extended the number of channels to be considered occupied by adding adjacent unoccupied channels to more realistically reflect data loss from data flagging algorithms. Figure 3 shows an example for the same C-band spectrum above indicating what would be considered occupied vs unoccupied in the standard case and the more realistic extended case. In this example, the difference it makes is only 0.6%. In subsequent analysis this more realistic occupancy value is used. It is clear though that with this method only bright signals are picked up for occupancy and weaker signals are missed that fall below the determined threshold. While this weaker interference can still affect astronomical data and their impact is not negligible, especially for deep integrations, bright signals can more significantly affect the ability to calibrate with on-sky sources and have a stronger effect on generated image fidelity and potentially reduce the usable bandwidth and overall sensitivity of the instrument when integrating over usable bandwidth and time. In this example, the lowest spectral window of the frequency range, 4 000–4 200 MHz is dominated by interference from the C-band geostationary satellite downlink band that is primarily used by Cable TV networks and radio stations to provide programming.

4 Results

4.1 General Trends

In the following spectral occupancy trends between 2013 and 2026 are presented broken down by VLA receiver. In addition, Table 2 provides a comparison of spectral occupancy values between 2013 and 2026 per VLA receiver band.

P-band (224–480 MHz)

The current VLA P-band system came online for observing semester 2013B (September 2013 - January 2014). It was added to the VLA regular RFI survey scans in July 2015. Figure 4 shows the spectral

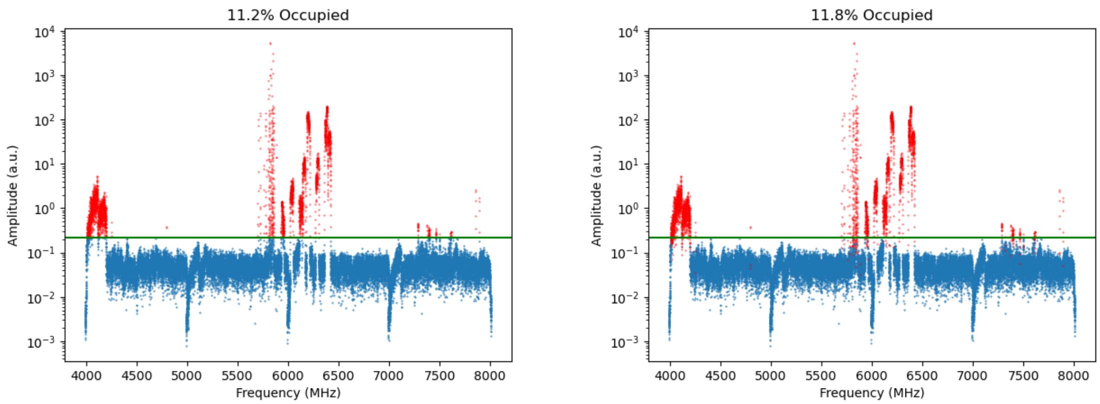

Figure 3: *Left:* Vector averaged spectrum, red points are considered occupied, blue points are considered unoccupied channels, the green line indicates the chosen noise threshold. *Right: The same as on the left with the exception that occupied channels are grown to adjacent unoccupied channels.*

occupancy since 2015 primarily for the NCP pointing, the data for P-band in almost all of the southern pointings were flagged. The spectral occupancy for the VLA at P-band has a median of 32% with an overall trend (least squares linear fit) in the past 10 years of 0.19±0.14% increase per year, meaning that spectral occupancy has increased by about 1.9±1.4% at P-band taking only the fixed VLA configuration independent baselines into account. The rms of the data is 0.33% and the standard deviation is 3.1%. Overall, this shows the spectral occupancy at P-band was relatively stable over the past decade.

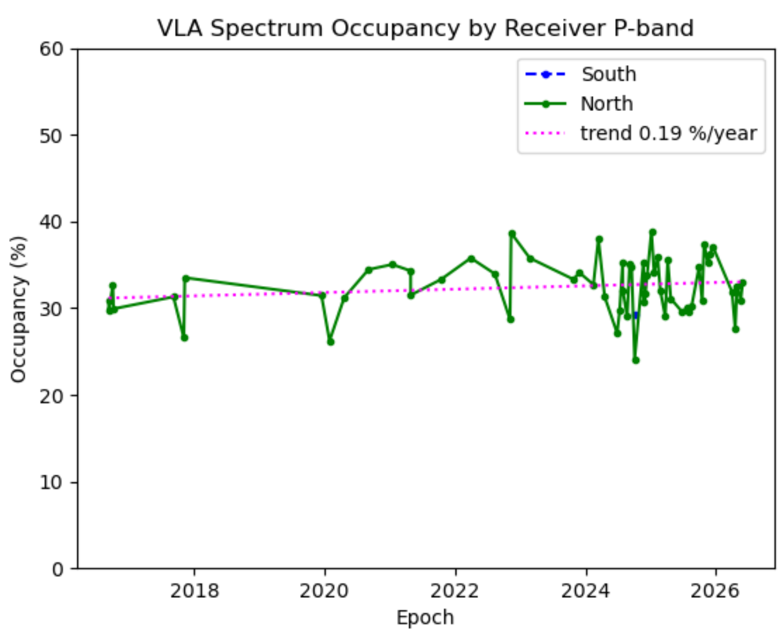

Figure 4: Spectral occupancy between 2016 and 2026 for P-band `rfisurvey` observations.

L-band (1 000–2 000 MHz)

The current VLA L-band system became fully available after the EVLA upgrade completed around 2012, together with the other >1 000 MHz receivers. The trend from 2013 until mid-2026 is shown in Figure 6.

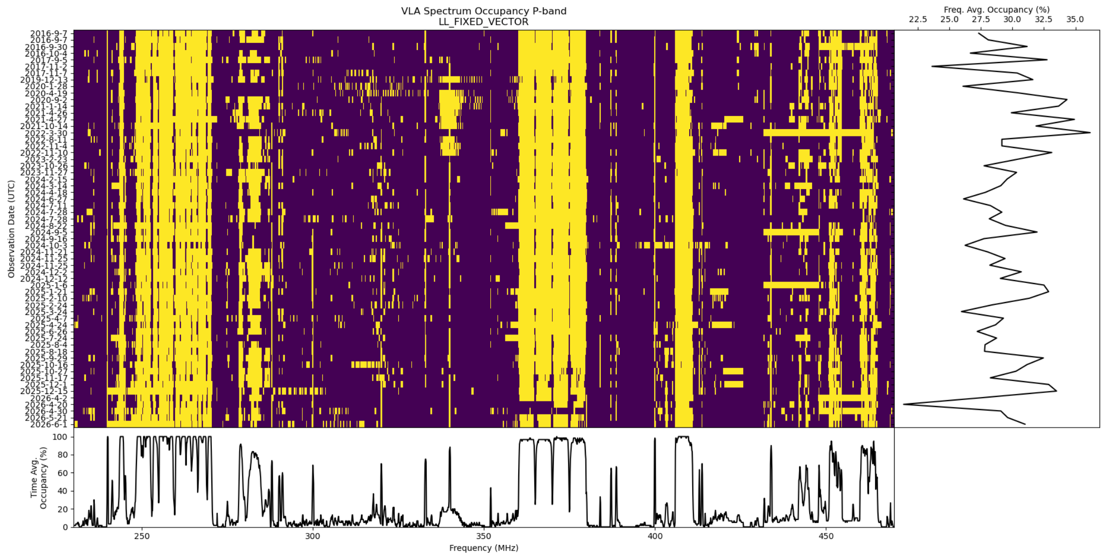

Figure 5: (Main) Waterfall plot showing spectral occupancy for P-band. (Bottom) Time averaged spectral occupancy. (Right) Frequency/Band averaged spectral occupancy. Data from the YY correlation product for all fixed antenna NCP observations.

A linear trend for this time period indicates an increase in spectral occupancy of 0.77±0.11%/year and a median spectral occupancy of 35% for the configuration independent baselines. The rms was 3.5% and the standard deviation was 3.8%. The low point outlier around 2017 is explained with the transition to GOES-R series[4] of NOAA weather satellites. The peak seen in 2026 was due the technology upgrade of a nearby cell-tower that increased the use of uplink frequencies at L-band, while providing downlink communication channels that both fell into L and S-band. The S-band transmitter toward the VLA was turned-off, thus the drop in occupancy, however the baseline spectral occupancy remained elevated due to the remaining up- and downlink channels that continued to broadcast due to the technology upgrade. For more information on this topic please refer to Lawson et al. (2026).

S-band (2 000–4 000 MHz)

The trend from 2013 until mid-2016 is shown in Figure 8. The median spectral occupancy for the fixed set of antennas is 22.7% with a standard deviation of 3.9%. A linear trend for this time period indicates an increase in spectral occupancy of 0.19±0.15% per year, which makes an overall increase by 1.9±1.5% over a decade. Again the impact, especially strongly pronounced in the Southern pointing shows again the activation and deactivation of cell-tower signals as described in Lawson et al. (2026). S-band is particularly impacted by satellite communications at the lower and upper end of the spectrum, in particular Sirius XM satellite transmissions that are picked up in the sidelobes. The rms of the distribution is 22% due to strong variability in received transmissions at different snapshots in time.

C-band (4 000–8 000 MHz)

The spectral occupancy at C-band shows a steady rise between 2013 and 2026, as can be seen in Figure 10. The steady steady rate of increase is 0.422±0.062%/year, making 4.2±0.6% over a decade. The median spectral occupancy is 11.6% with a standard deviations of 2.2% and a rms of 11.8%.

X-band (8.0–12.0 GHz)

The trend from 2013–2026 for X-band is shown in Figure 12. Spectral occupancy has been relatively steady up until 2023 when some datasets shows significant and highly variable increases in spectral occupancy. While a linear trend is not necessarily the best representation of this increase, it does reflect

[4]GOES-R is the fourth generation of the Geostationary Operational Environmental Satellite (GOES)

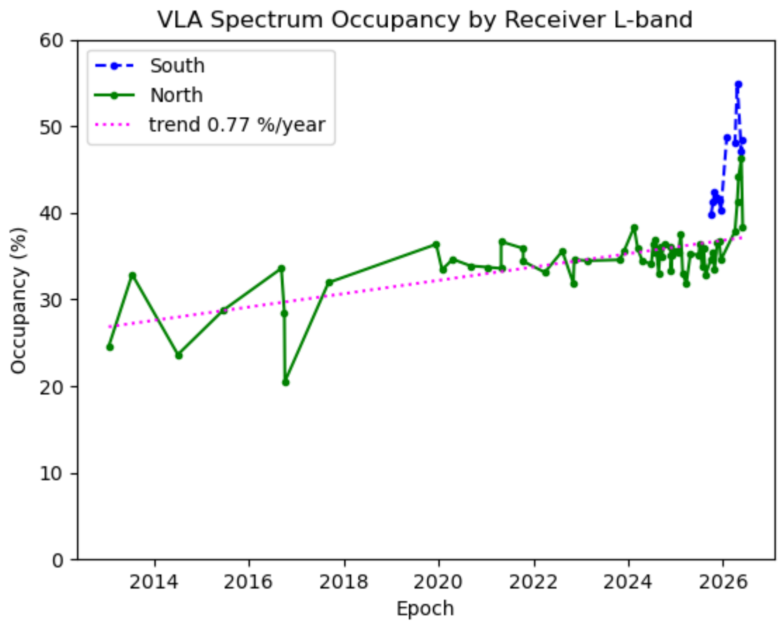

Figure 6: Spectral occupancy between 2013 and 2026 for L-band `rfisurvey` observations.

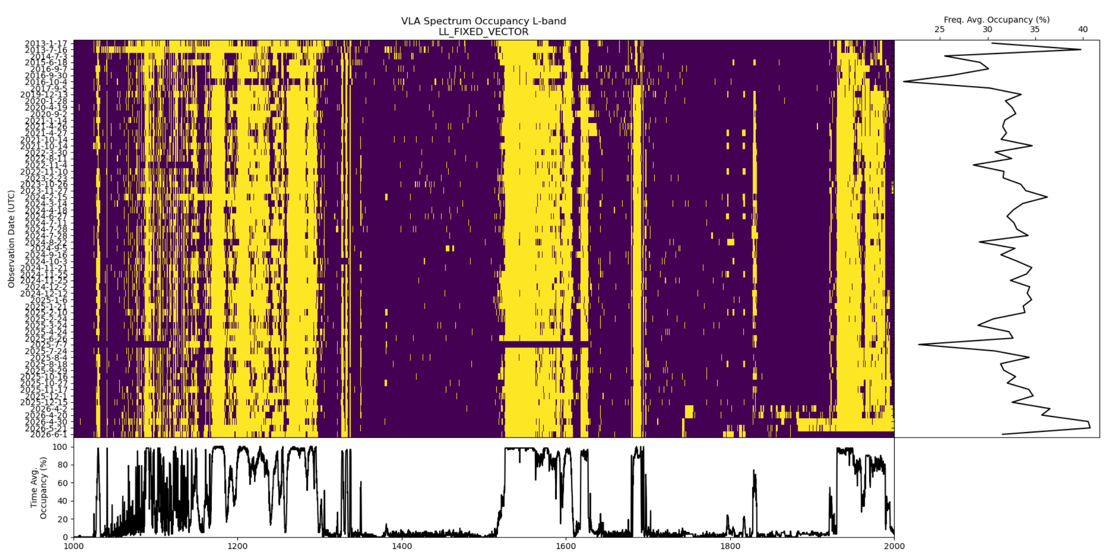

Figure 7: (Main) Waterfall plot showing spectral occupancy for L-band. (Bottom) Time averaged spectral occupancy. (Right) Frequency/Band averaged spectral occupancy. Data from the LL correlation product for all fixed antenna NCP observations.

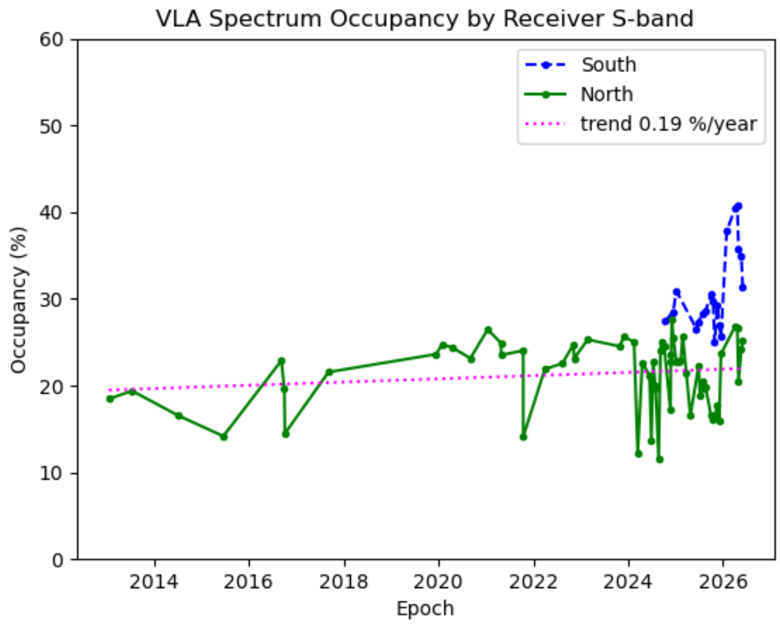

Figure 8: Spectral occupancy between 2013 and 2026 for S-band `rfisurvey` observations.

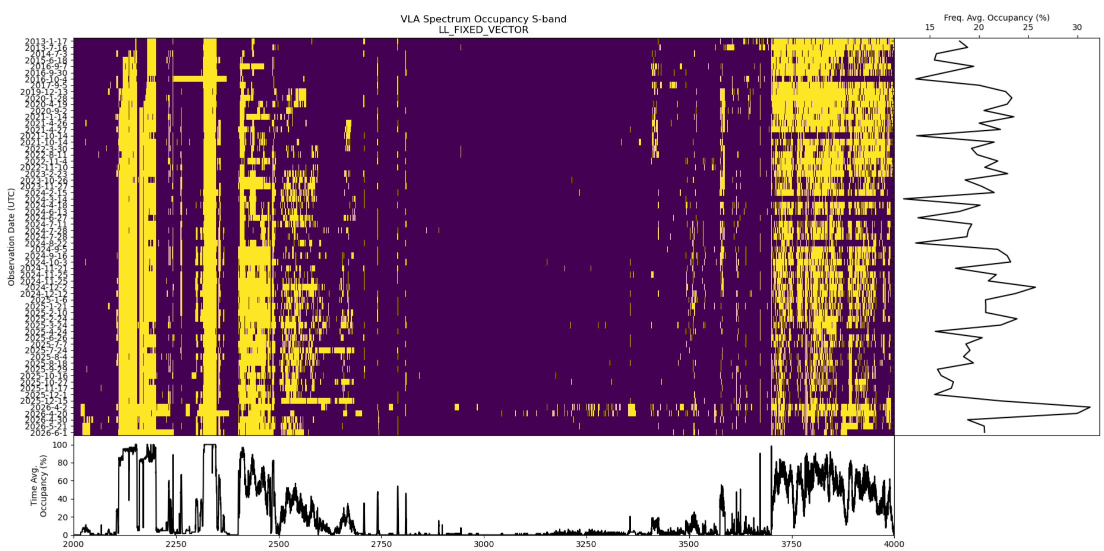

Figure 9: (Main) Waterfall plot showing spectral occupancy for S-band. (Bottom) Time averaged spectral occupancy. (Right) Frequency/Band averaged spectral occupancy. Data from the LL correlation product for all fixed antenna NCP observations.

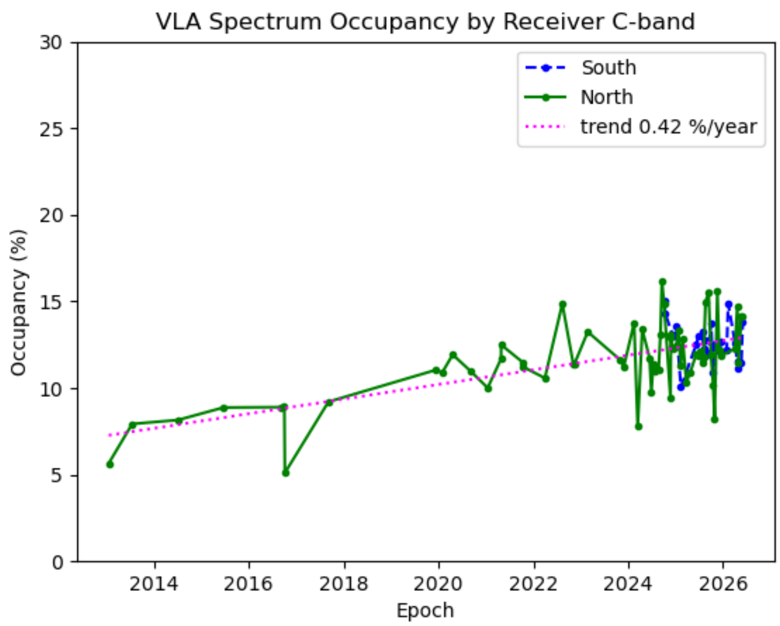

Figure 10: Spectral occupancy between 2013 and 2026 for C-band `rfisurvey` observations.

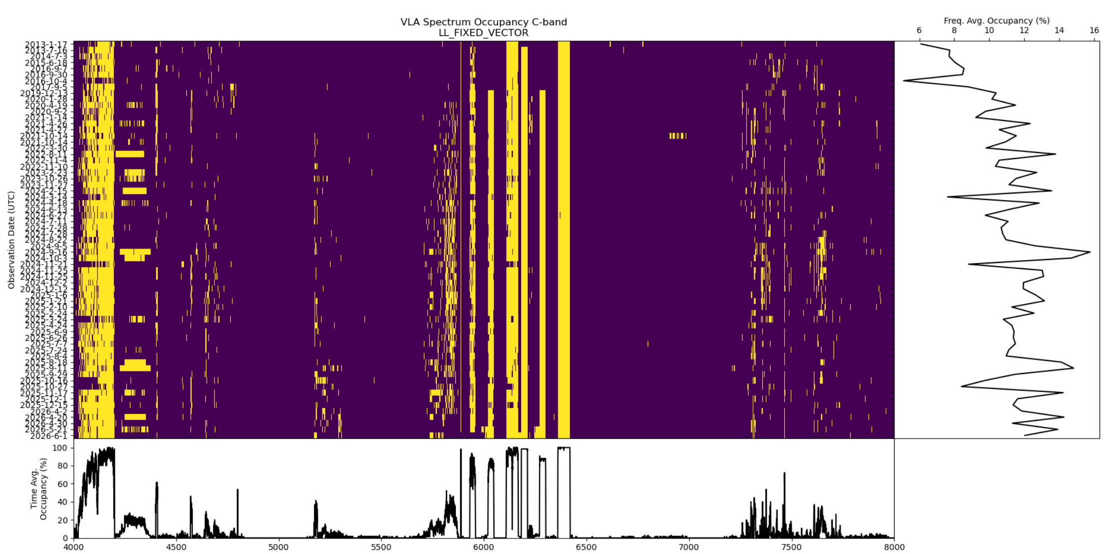

Figure 11: (Main) Waterfall plot showing spectral occupancy for C-band. (Bottom) Time averaged spectral occupancy. (Right) Frequency/Band averaged spectral occupancy. Data from the LL correlation product for all fixed antenna NCP observations.

the average mean change for that time period. The slope comes to 0.138±0.058% with a median of 1.3%, a standard deviation of 1.6%, and a rms of 2.5%. Also note that the Southern pointing shows higher spectral occupancy as compared to the Northern Celestial Pole with a median occupancy of 6.3±2.1% as compared to 2.2±1.8% for the Northern pointing covering the same time period.

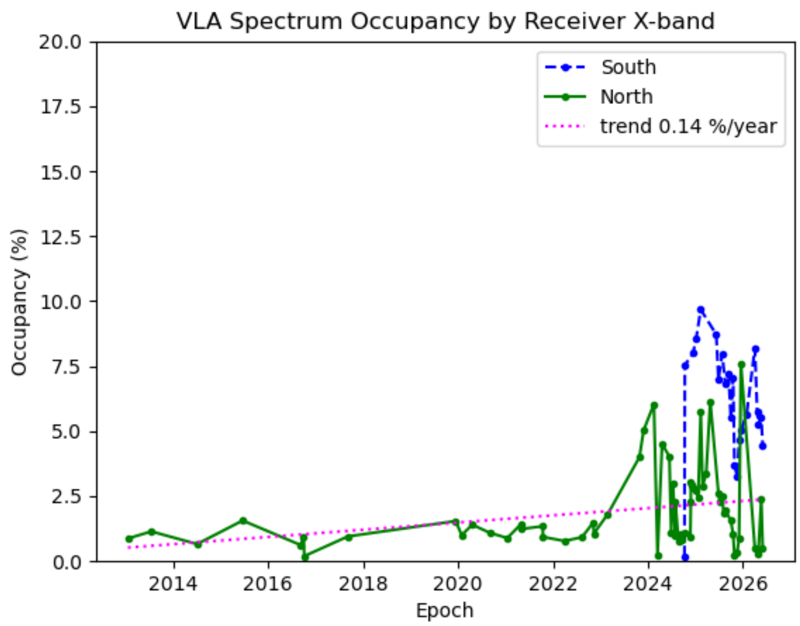

Figure 12: Spectral occupancy between 2013 and 2026 for X-band `rfisurvey` observations.

Ku-band (12.0–18.0 GHz)

The trend for Ku-band is shown in Figure 14, where it can be seen that overall spectral occupancy has been steady over the past decade. The median spectral occupancy for the Northern pointing between 2013 and 2026 was 7.8±1.3% and for the Southern sky pointing it was 9.78±0.68%. The rms of the Northern pointing was 7.5%, primarily driven by larger variability in observations since 2024.

K, Ka, Q bands (18.0–50.0 GHz)

For K (18.0–26.5 GHz), the spectral occupancy over the past decade was dominated by emission in the lower part of the band, as can be seen in Figure 17. The median spectral occupancy for the Northern pointing was 1.1±0.6% and for the Southern pointing it was 5.9±0.7%. For Ka (26.5–40.0 GHz), and Q (40.0–50.0 GHz) bands the spectral occupancy over the past decade was 0% with only one outlier in Q-band. Similarly, since 2024 the Southern pointing also showed no occupied channels at these bands. The occupancy vs time plots for these three bands are combined in Figure 16.

For a better presentation of the long-term occupancy trends across this wide spectral range, individual spectral windows of 128 MHz bandwidth each are used to determine frequency dependent occupancy values. The resulting data is shown in a waterfall type diagram in Figure 20 and illustrates spectral hot-spots where radio astronomical observations are either impossible or require sophisticated ways to be able to detect faint emissions of cosmic origin. For P-band 16 MHz wide spectral windows were used and the corresponding waterfall representation is presented in Figure 21.

Finally, the median spectral occupancy is tabulated for each receiver band for two distinct points in time. The data between 2013 and 2016 was combined to obtain a rough picture of what the spectral usage detected by the VLA was around that time and compare it to the current environment by combining all available data from 2026 for the Northern Celestial Pole pointing. The results of this analysis are shown in Table 2. In addition, with the recent addition of a Southern pointing, the values for 2026 datasets is

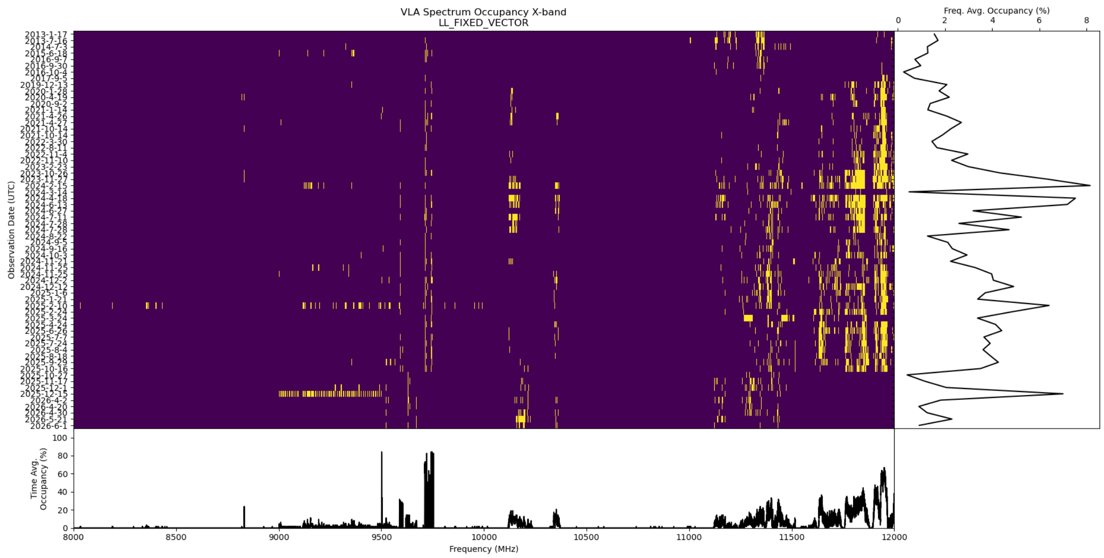

Figure 13: (Main) Waterfall plot showing spectral occupancy for X-band. (Bottom) Time averaged spectral occupancy. (Right) Frequency/Band averaged spectral occupancy. Data from the LL correlation product for all fixed antenna NCP observations.

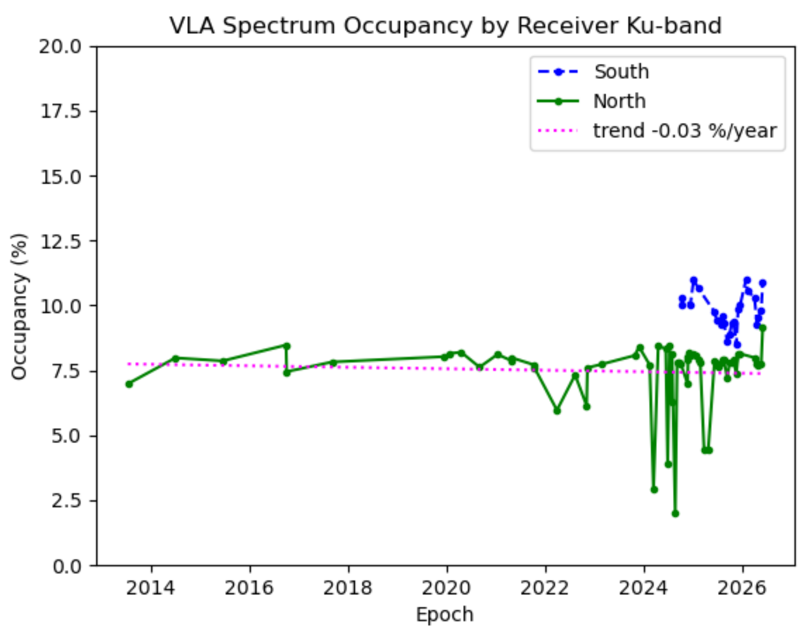

Figure 14: Spectral occupancy between 2013 and 2026 for Ku-band `rfisurvey` observations.

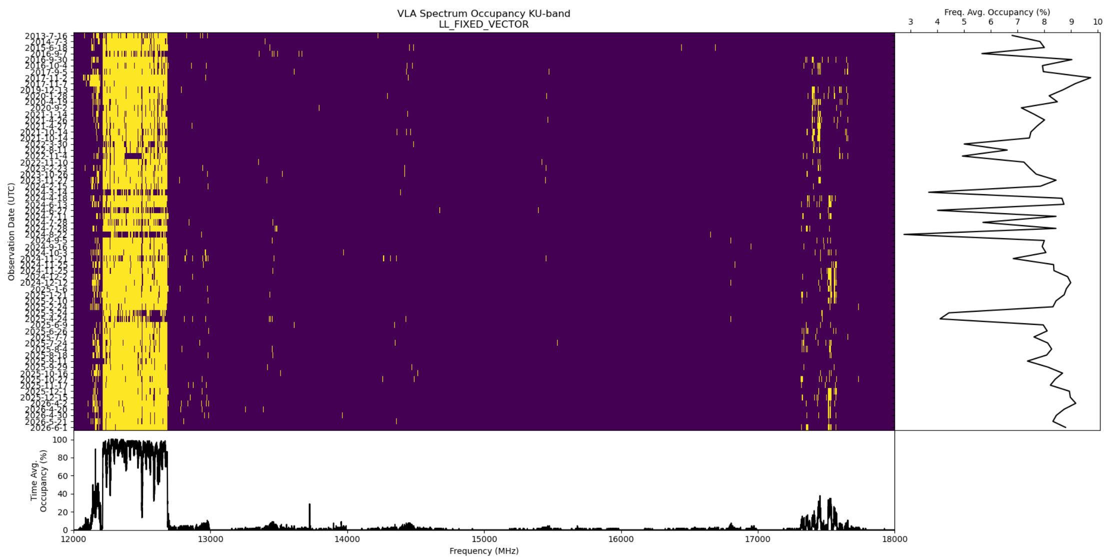

Figure 15: (Main) Waterfall plot showing spectral occupancy for Ku-band. (Bottom) Time averaged spectral occupancy. (Right) Frequency/Band averaged spectral occupancy. Data from the LL correlation product for all fixed antenna NCP observations.

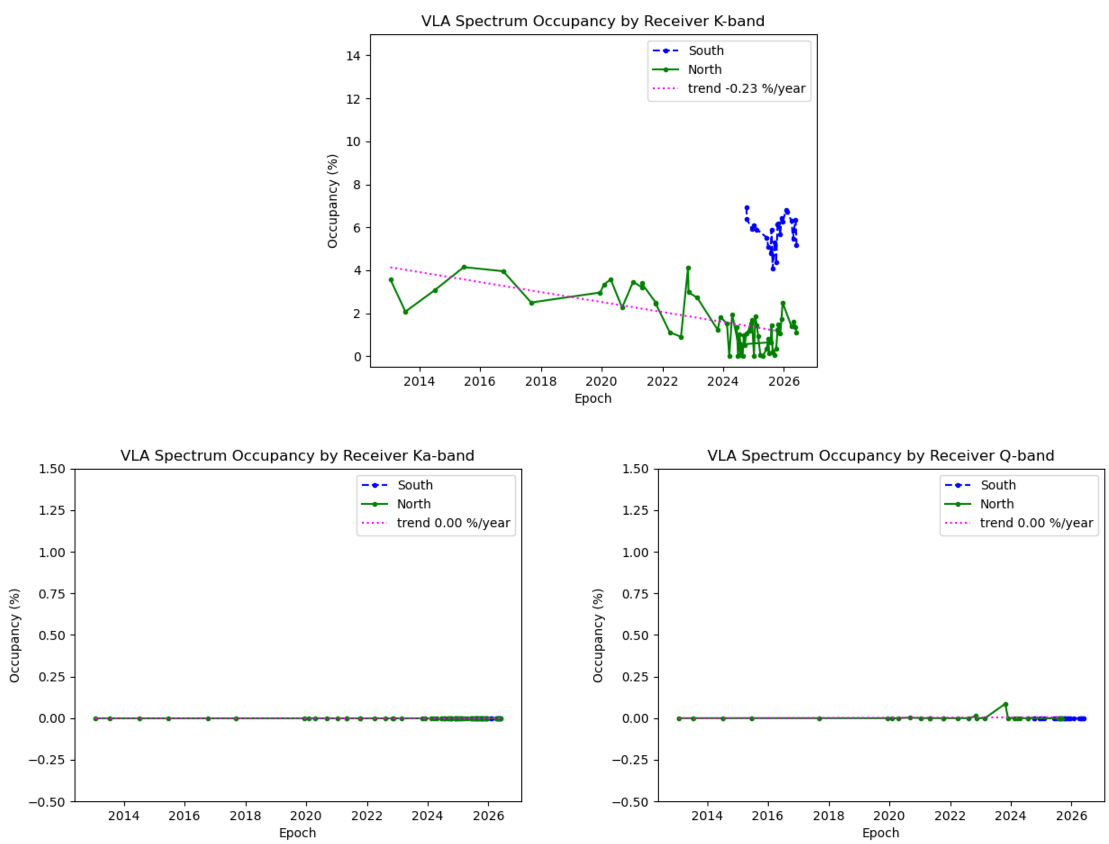

Figure 16: Top: Spectral occupancy between 2013 and 2026 for K-band `rfisurvey` observations. Bottom Left: Spectral occupancy between 2013 and 2026 for Ka-band `rfisurvey` observations. Bottom Right: Spectral occupancy between 2013 and 2026 for Q-band `rfisurvey` observations.

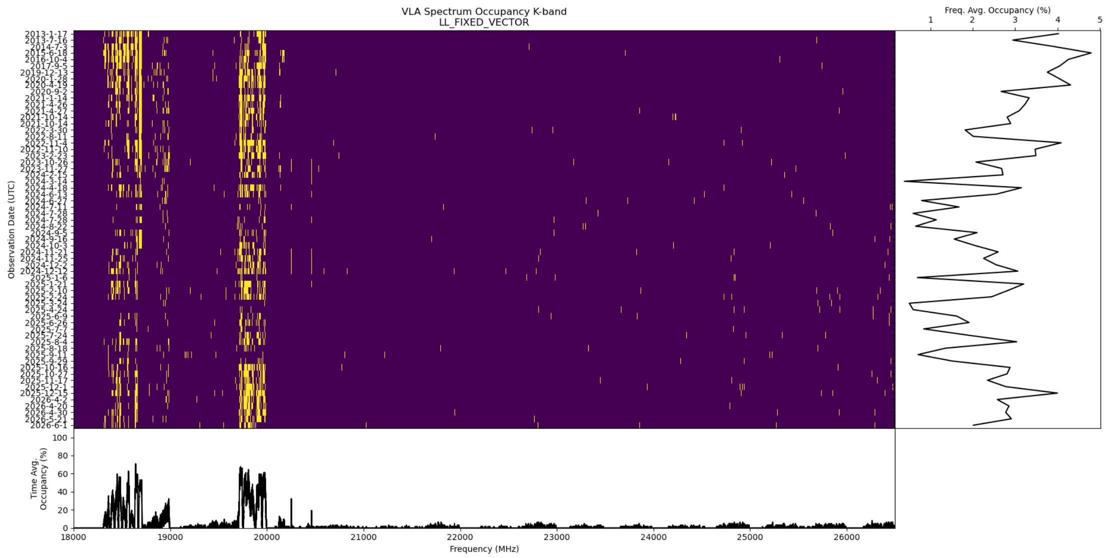

Figure 17: (Main) Waterfall plot showing spectral occupancy for K-band. (Bottom) Time averaged spectral occupancy. (Right) Frequency/Band averaged spectral occupancy. Data from the LL correlation product for all fixed antenna NCP observations.

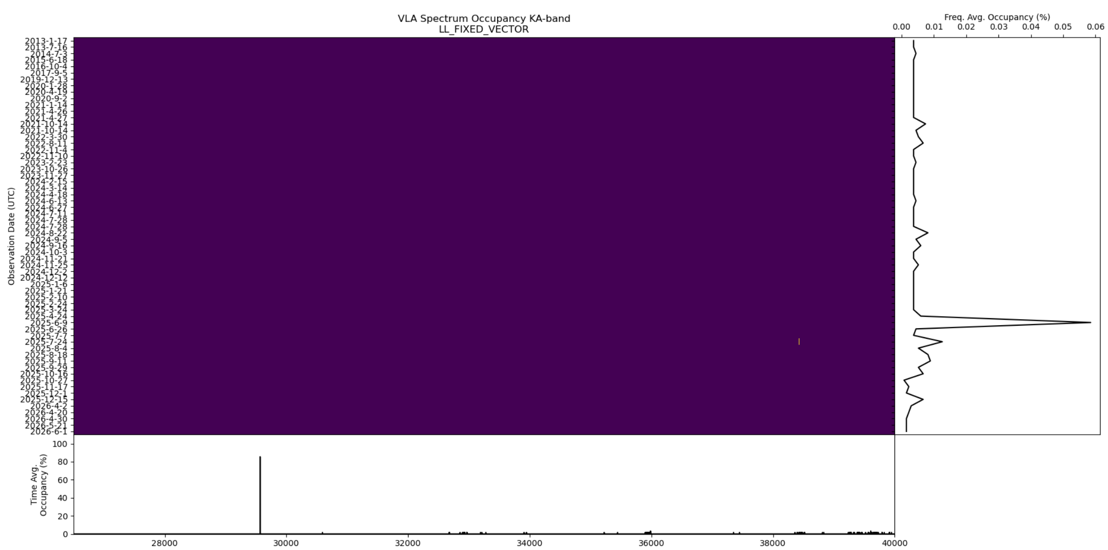

Figure 18: (Main) Waterfall plot showing spectral occupancy for Ka-band. (Bottom) Time averaged spectral occupancy. (Right) Frequency/Band averaged spectral occupancy. Data from the LL correlation product for all fixed antenna NCP observations.

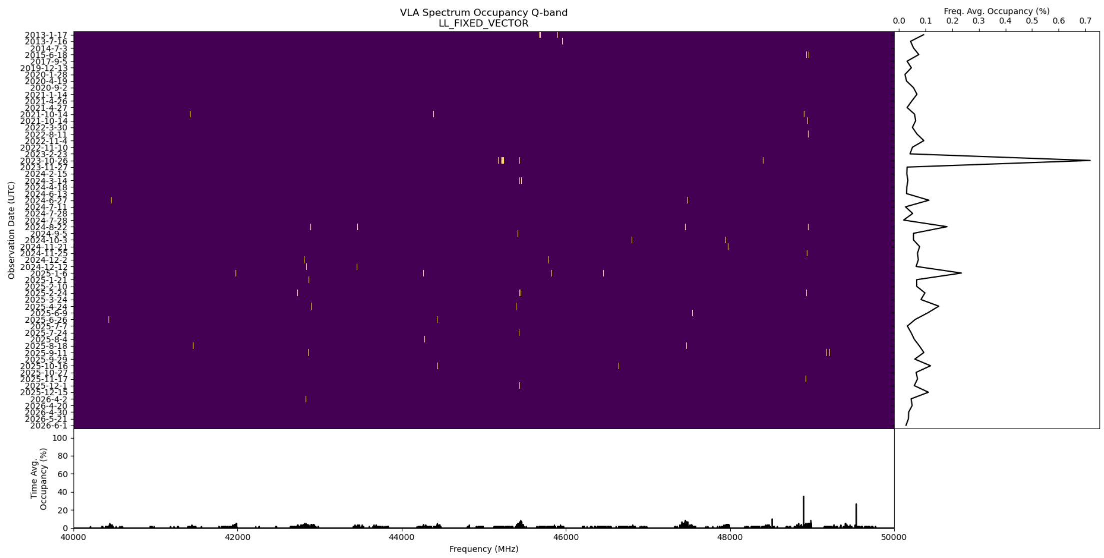

Figure 19: (Main) Waterfall plot showing spectral occupancy for Q-band. (Bottom) Time averaged spectral occupancy. (Right) Frequency/Band averaged spectral occupancy. Data from the LL correlation product for all fixed antenna NCP observations.

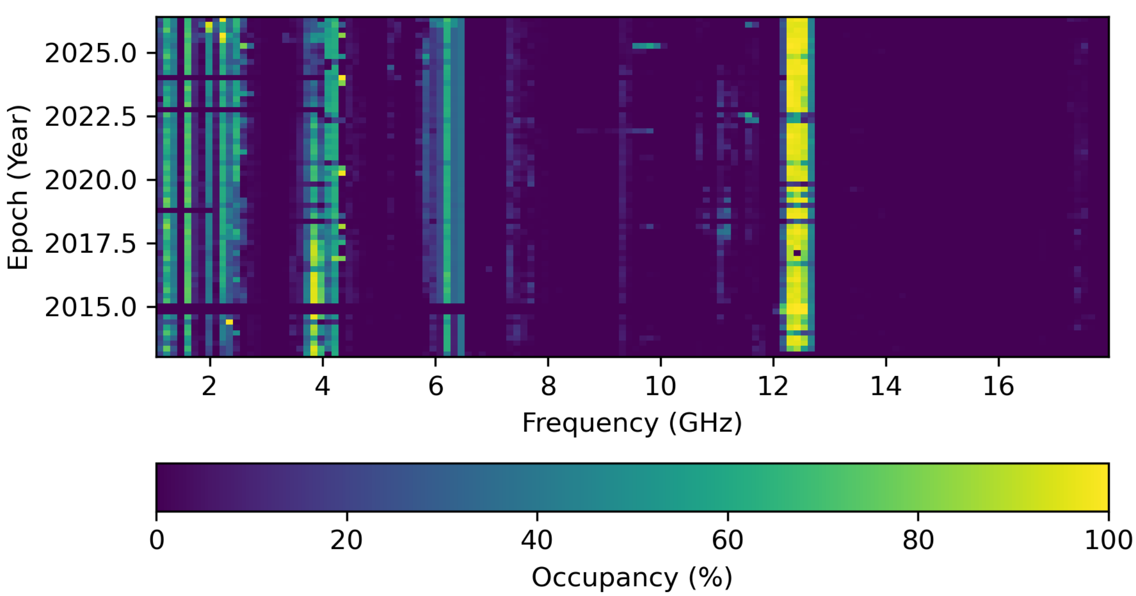

Figure 20: Spectral occupancy between 2013 and 2026 for 1–18 GHz `rfisurvey` Northern Celestial Pole observations for each 128 MHz spectral window. If for technical reason occupancy was not able to be determined for a particular band or spectral window, a 0 value is shown in this plot.

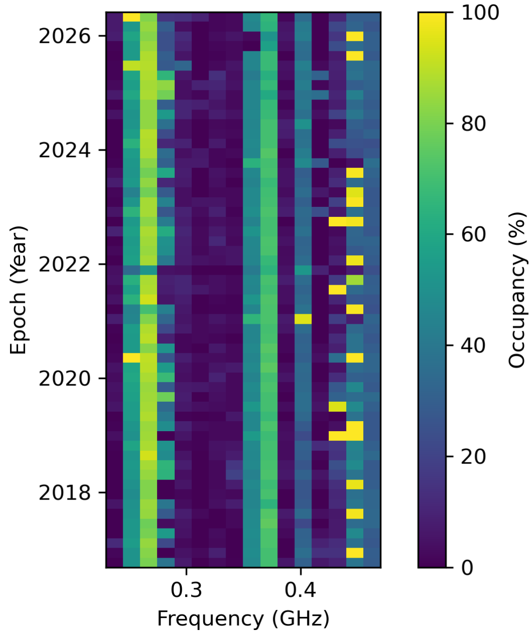

Figure 21: Spectral occupancy between 2017 and 2026 for 200–500 MHz `rfisurvey` Northern Celestial Pole observations for each 16 MHz spectral window. If for technical reason occupancy was not able to be determined for a particular band or spectral window, a 0 value is shown in this plot.

also tabulated. Overall, this shows that over a decade the loss in usable bandwidth is about 145 MHz at L-band, 152 MHz at S-band, 244 MHz at C-band, and 204 MHz at X-band, while Ku, K, Ka,and Q saw little to no change over that time period.

Table 2: Spectral occupancy snapshots between 2013–2016 (in case of P-band 2017) and 2026 for VLA observations pointing to the Northern Celestial Pole (N) and 2026 Observations pointing South (S). The errors are the standard deviation of the data.

RX	Range (GHz)	2013–2016 (%)	2026 N (%)	2026 S (%)	Δt (%)	ΔN-S (%)
L	1.0–2.0	26.7±3.7	41.2±3.3	48.4±2.8	14.5±5.0	-7.2±4.3
S	2.0–4.0	17.5±2.0	25.1±2.3	36.8±3.3	7.6±3.0	-11.7±4.0
C	4.0–8.0	8.0±1.2	14.1±1.3	12.2±1.3	6.1±1.8	1.9±1.8
X	8.0–12.0	1.01±0.34	0.50±0.79	5.6±1.1	-0.5±1.8	-5.1±1.4
Ku	12.0–18.0	7.86±0.45	7.76±0.56	10.27±0.62	-0.1±0.72	-2.51±0.84
K	18.0–26.5	2.9±0.8	0.95±0.16	6.29±0.58	-1.95±0.82	-5.34±0.60
Ka	26.5–40.0	0	0	0	-	-
Q	40.0–50.0	0	0	0	-	-
		2017 (%)	2026 (%)			
P	0.2–0.5	30.4±1.2	32.9±1.9	n/a	2.5±2.2	n/a

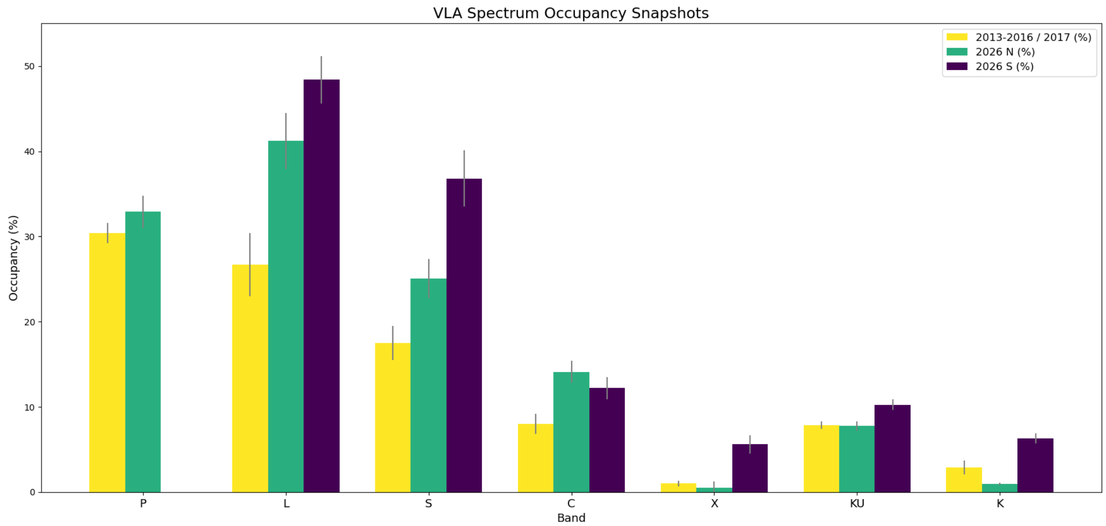

Figure 22: Visualization of the occupancy snapshots in Table 2.

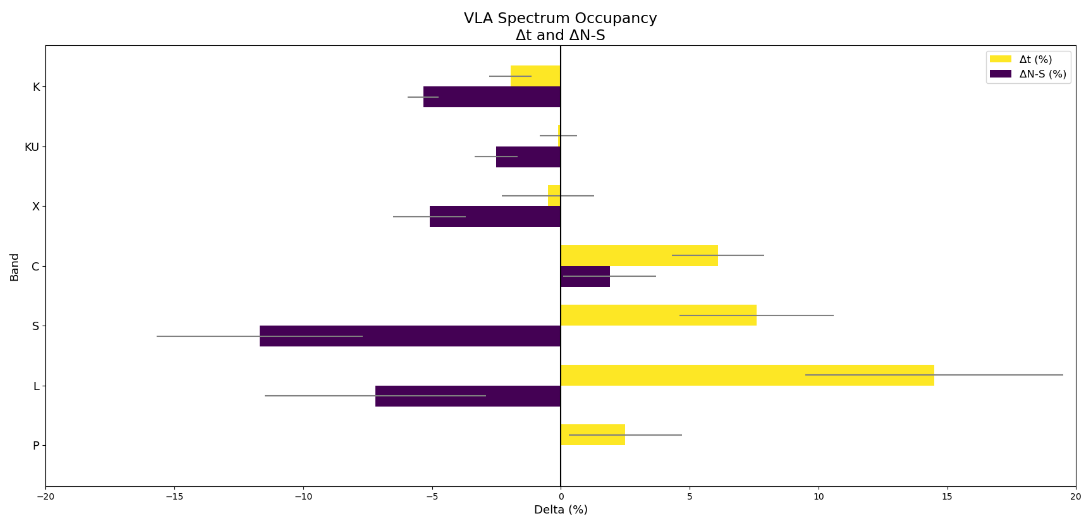

Figure 23: Visualization of the deltas presented in Table 2. Yellow bars stretching to the right of the plot represent occupancy increasing in time. Purple bars stretching to the left of the plot represent data taken from the Southern pointing being more occupied than the NCP pointing.

4.2 VLA Configuration Based Trends

Since the VLA is an interferometer, it acts as a spatial filter and radio frequency interference appears differently in data based on baseline lengths and with respect to the location of the transmitter. With the VLA antenna locations reconfigurable, there are four different configurations realized through a cycle of 15 months with the longest baselines ranging from 1.03 to 36.4 km and the shortest baselines ranging from 35 to 680 m. The four configurations are labeled A (36.4 km / 680 m),B (11.1 km / 210 m),C (3.4 km / 35.5 m), D (1.03 km/35 m) in decreasing baseline length. In this section the effect of baseline length on spectral occupancy is analyzed per receiver band and configuration using the longest and the shortest

Table 3: Spectral occupancy in % using the Northern Celestial Pole pointing for four different VLA configurations. For each configuration the shortest and longest baseline lengths are given.

RX	P (%)	L (%)	S (%)	C (%)	X (%)	Ku (%)
	A Configuration (36.4 km / 680 m)					
Short	31.9±1.9	41.2±3.3	25.0±2.3	14.10±1.3	0.50±0.79	7.76±0.56
Long	20.4±2.0	12.98±0.73	3.72±0.0042	0.053±0.14	0	0.026±0.013
Avg.	32.0±1.6	33.2±1.8	16.0±1.7	9.03±1.5	0.14 ± 0.045	0.81±0.51
	B Configuration (11.1 km / 210 m)					
Short	38.9±2.9	40.1±1.2	18.1±2.2	15.6±1.4	3.9±3.5	10.57±0.23
Long	27.6±2.8	13.31±0.67	5.34±0.69	3.34±0.82	0.27±2.6	0.5±2.4
Avg.	38.6±3.0	35.0±1.6	13.7±2.9	11.4±1.4	0.94±2.6	7.39±0.34
	C Configuration (3.4 km / 35 m)					
Short	42.3±2.2	40.9±2.6	25.98±0.67	16.03±0.70	5.4±1.2	9.52±0.45
Long	27.71±0.67	21.0±2.0	10.91±0.88	7.56±0.49	0.450±0.074	7.16±0.31
Avg.	37.5±3.2	39.6±2.5	22.45±0.58	13.52±0.24	5.8±2.5	8.20±0.01
	D Configuration (1.03 km / 35 m)					
Short	37.89±0.36	37.6±2.0	30.1±1.4	16.20±0.72	20.1±3.5	11.3±1.1
Long	35.2±5.9	34.8±1.9	22.4±1.3	9.55±0.44	2.3±1.2	8.64±0.44
Avg.	32.8±3.3	40.78±0.28	31.1±2.4	15.61±0.88	15.0±3.6	10.38±0.52

baselines triangles in each observation.

Here the data taken during the latest four VLA configurations is taken to characterize the impact of baseline length has on the spectral occupancy in each band below 18 GHz. The date range for A configuration was Feb 20 2026–Jun 22 2026, B configuration was Sep 03 2025–Jan 20 2026, C configuration lasted from May 22 2025–Aug 28 2025, and D configuration lasted from Feb 25 2025–May 12 2025. The resulting occupancy values for shortest and longest baseline triangles, as well as the average of all available baselines (nominally 351) of the array, are presented in Table 3 for NCP pointing and Table 4 for the Southern pointing. No dataset was available for the Southern pointing in D configuration at the date of writing. A future revision of this memo could fill the missing data with new observations. These values might be considered or compared to what is currently recommended to VLA users.

4.3 NTIA Study Bands

During 2025 the NTIA was tasked to study federal frequency allocations for the possibility of making these available for high power commercial wireless use. The specific frequency ranges of interest for these studies are 1 680–1 695, 2 690–2 900, 4 400–4 940, and 7 125–7 400 MHz. In addition, wireless spectrum is planned to be auctioned imminently for the 3 980–4 200 MHz band. Therefore, we include here a past and current band occupancy analysis for the VLA RFI sweeps that provide a past and current picture of band usage that will become available for commercial use in the coming 10 years and that have the potential to impact opportunistic radio astronomical observations in those frequency ranges.

1 680–1 695 MHz

This band is primarily used for space-to-Earth transmissions from GOES-R satellites and has utilized this band at almost 100% occupancy since GOES-R series satellites went online. Figure 26 shows the band usage as observed from the VLA from 2013 to now. For the NCP pointing the band has

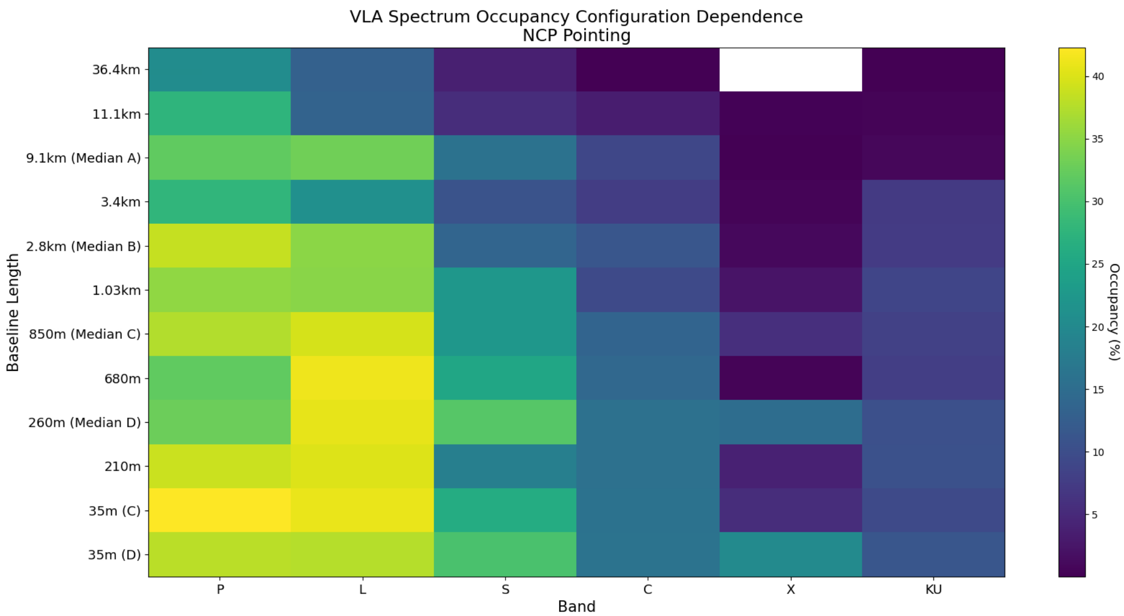

Figure 24: Visualization of data from Table 3.

Table 4: Spectral occupancy in % using the Southern pointing for four different VLA configurations. For each configuration the shortest and longest baseline lengths are given.

RX	**L** (%)	**S** (%)	**C** (%)	**X** (%)	**Ku** (%)
		A Configuration (36.4 km / 680 m)			
Short	48.2±3.1	37.7±3.9	12.07±0.97	5.6±1.4	10.04±0.59
Long	27.0±2.7	8.0±1.1	0	3.41±0.63	0.11±0.44
Avg.	47.1±3.6	28.3±3.0	9.84±0.21	0.40±0.52	8.23±0.29
		B Configuration (11.1 km / 210 m)			
Short	50.1±5.2	28.9±1.9	14.0±1.1	5.2±1.7	10.68±0.29
Long	16.5±3.8	5.81±0.33	8.21±0.25	0.45±0.50	4.55±0.97
Avg.	45.6±3.5	27.49±0.55	13.31±0.84	2.1±1.2	9.20±0.10
		C Configuration (3.4 km / 35 m)			
Short	-	31.8±1.1	13.1±3.2	8.17±0.85	10.2±3.5
Long	-	20.48±0.60	2.66±0.87	3.24±0.48	8.41±0.48
Avg.	-	31.86±0.21	10.3±2.6	7.83±0.29	9.83±0.26
		D Configuration (1.03 km / 35 m)			
Short	-	-	-	-	-
Long	-	-	-	-	-
Avg.	-	-	-	-	-

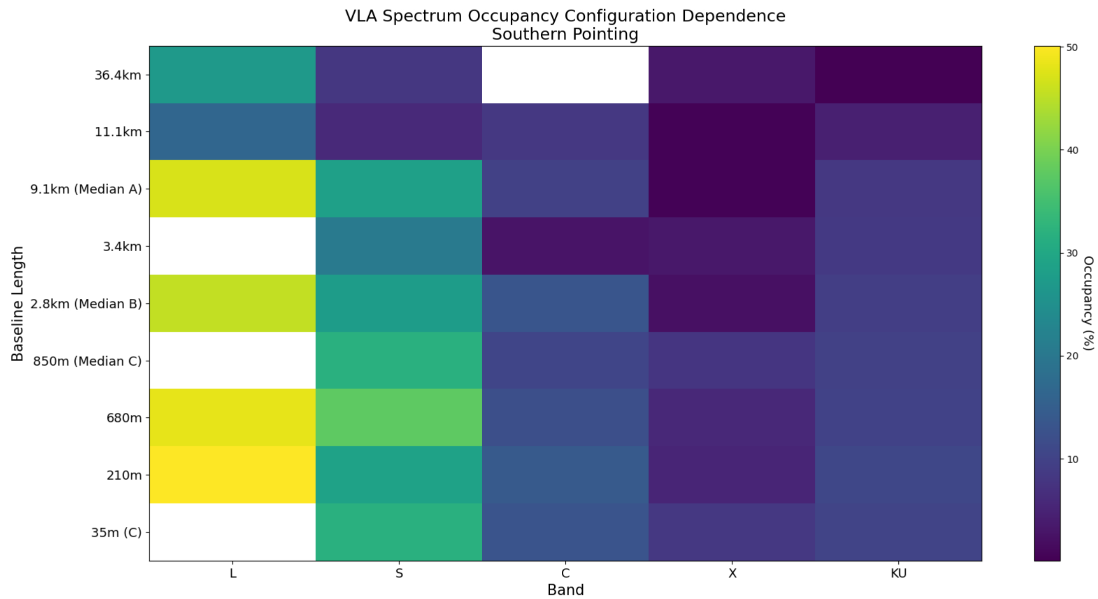

Figure 25: Visualization of data from Table 4.

been steadily occupied at 85.5±2.6% since about 2018. For the past year the Southern pointing shows a spectral occupancy of 92.5±4.8%. Therefore this band should be currently not accessible to radio astronomy from the ground.

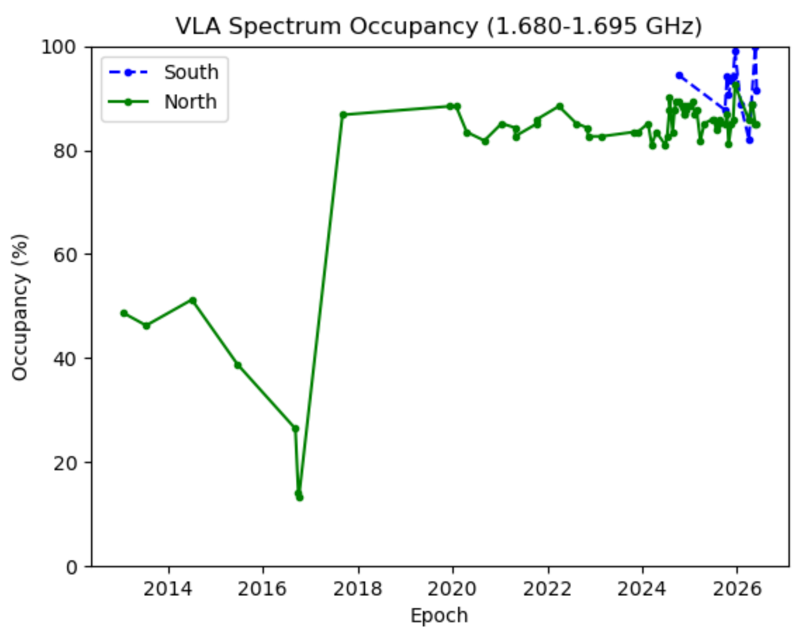

Figure 26: Study band 1 680–1 695 MHz spectral occupancy between 2013 and 2026. The change in spectral occupancy around 2017 coincides with the change to NOAA/NASA Geostationary Operational Environment Satellites R (GOES-R) series satellites that launched in 2016 and introduced wider bandwidth communications.

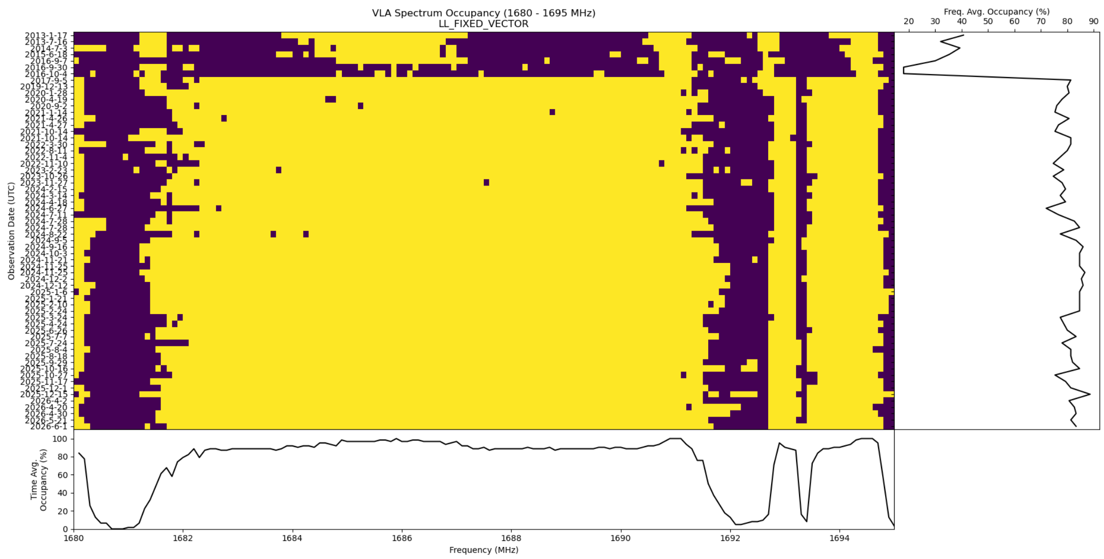

Figure 27: (Main) Waterfall plot showing spectral occupancy for the 1 680–1 695 MHz band. (Bottom) Time averaged spectral occupancy. (Right) Frequency/Band averaged spectral occupancy. Data from the LL correlation product for all fixed antenna NCP observations.

2 690–2 900 MHz

In the U.S. this band is primarily allocated for meteorological or aeronautical applications. Adjacent to this bands is one of the primary radio astronomy allocations (2 690–2 700 MHz) where all emissions are prohibited. At the VLA, as can be seen from Figure 28 the spectral occupancy is very low with a median value of 2.05±0.59% for NCP and 1.83±0.59% for the Southern pointing.

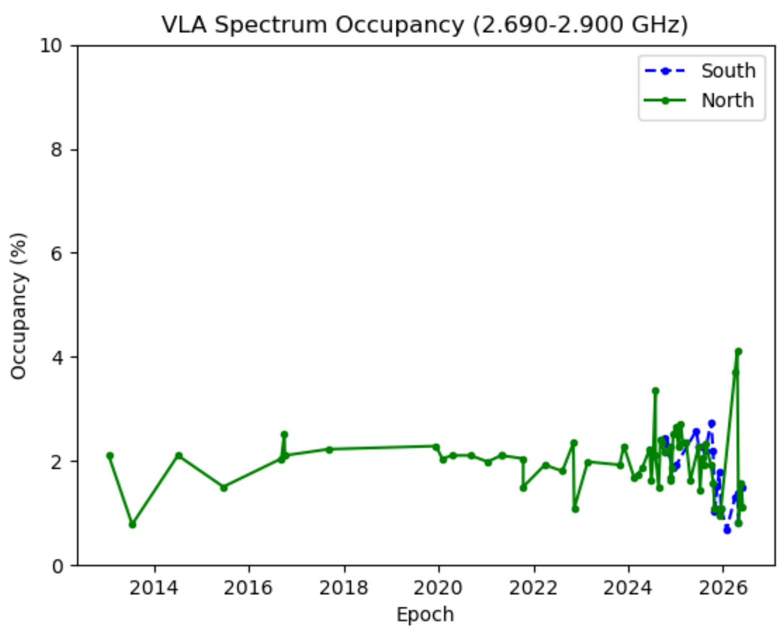

Figure 28: Study band 2 690–2 900 MHz spectral occupancy between 2013 and 2026.

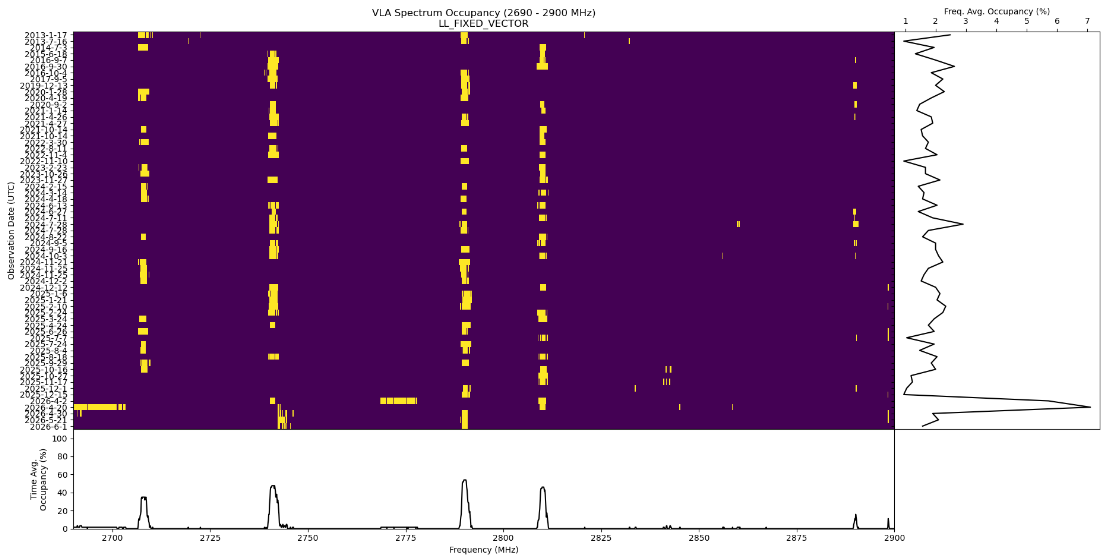

Figure 29: (Main) Waterfall plot showing spectral occupancy for the 2 690–2 900 MHz band. (Bottom) Time averaged spectral occupancy. (Right) Frequency/Band averaged spectral occupancy. Data from the LL correlation product for all fixed antenna NCP observations.

3 980–4 200 MHz

This band is already slated for auction for wireless communications use to augment Upper C band commercial wireless spectrum. It falls on the edge of the VLA S and C-band receivers and thus current measured occupancies are to be considered due to bandpass roll-off effects between the receiver bands. The lower half of the band falls into S-band from 3 980–4 011.25 MHz and the upper half falls into the C-band receiver 3 988.625–4 200 MHz. As can be seen in Figure 30 this is a very busy frequency range. The S-band median occupancy values are 14.0±17% for NCP and 42±11% for the Southern pointing with a significant dropping trend in the past years at least for the NCP pointing. For the C-band receiver range the median occupancy was relatively steady with 72±16 for NCP and 92.0±2.5%.

4 400–4 940 MHz

This band has different uses, e.g., 4 400–4 940 MHz in FCC'a Frequency Table of Allocations lists footnote US113, which states that radio astronomy observations of the formaldehyde line frequencies 4 825-4 835 MHz and 14.47-14.5 GHz may be made at certain radio astronomy observatories, including the VLA. Furthermore, every practicable effort will be made to avoid the assignment of frequencies to stations in the fixed or mobile services in these bands. Should such assignments result in harmful interference to these observations, the situation will be remedied to the extent practicable. As can be seen in Figure 32 shows little spectral use with the NCP pointing median average being 2.0±1.1% and the Southern pointing median being 3.0±1.1%.

7 125–7 400 MHz

This band is used by point-to-point links, satellite up- and downlinks and contains no radio astronomy allocations, nor are allocations adjacent to this band. Figure 34 shows the observed occupancy in VLA `rfisurvey` data. The median occupancy is 7.0±3.0% for NCP and 10.0±3.3%.

4.4 Special Bands of Interest

A number of frequency bands with widely common transmissions driven by modern communication needs are specifically looked at in the following section. These include the impacts from proliferation

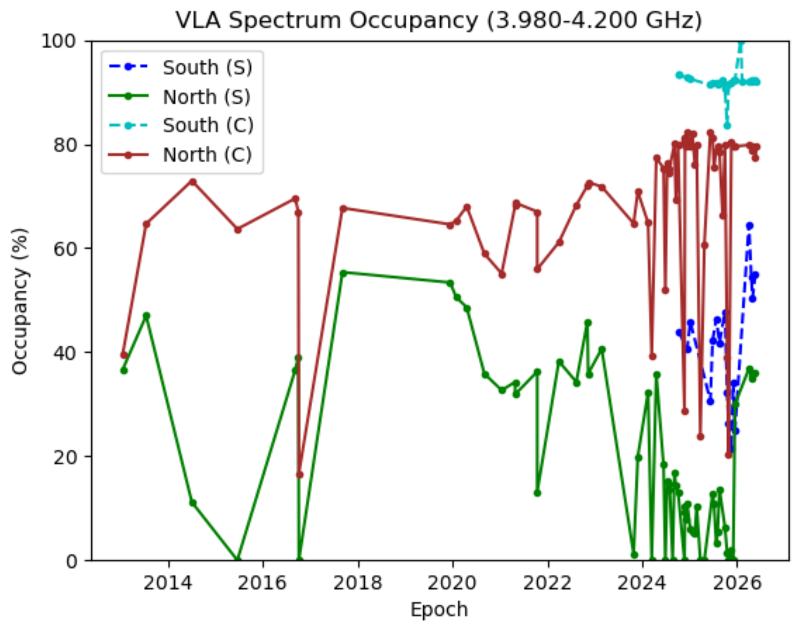

Figure 30: Study band 3.980–4.200 GHz spectral occupancy between 2013 and 2026. The band was split into two parts indicated with (S) and (C) for corresponding receiver band. The probed S-band range was 3 980–4 011.25 MHz and the C-band receiver range was 3 988.625–4 200 MHz.

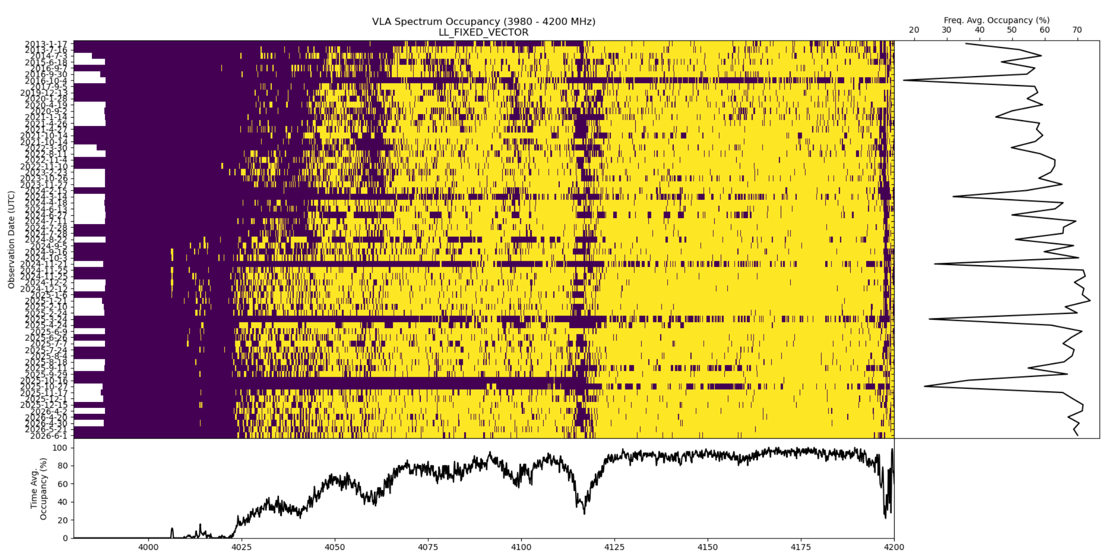

Figure 31: (Main) Waterfall plot showing spectral occupancy for the 3 980-4 200 MHz band using the C-band receiver. (Bottom) Time averaged spectral occupancy. (Right) Frequency/Band averaged spectral occupancy. Data from the LL correlation product for all fixed antenna NCP observations.

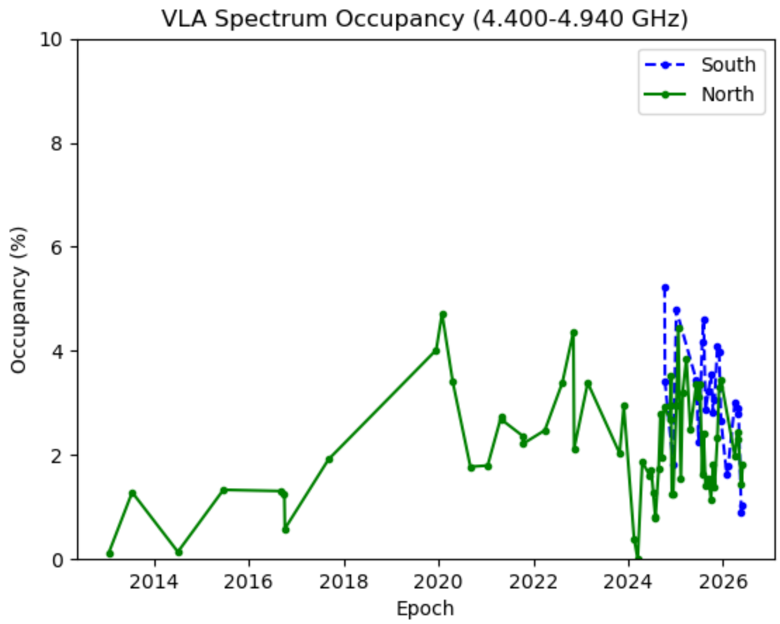

Figure 32: Study band 4 400–4 940 MHz spectral occupancy between 2013 and 2026.

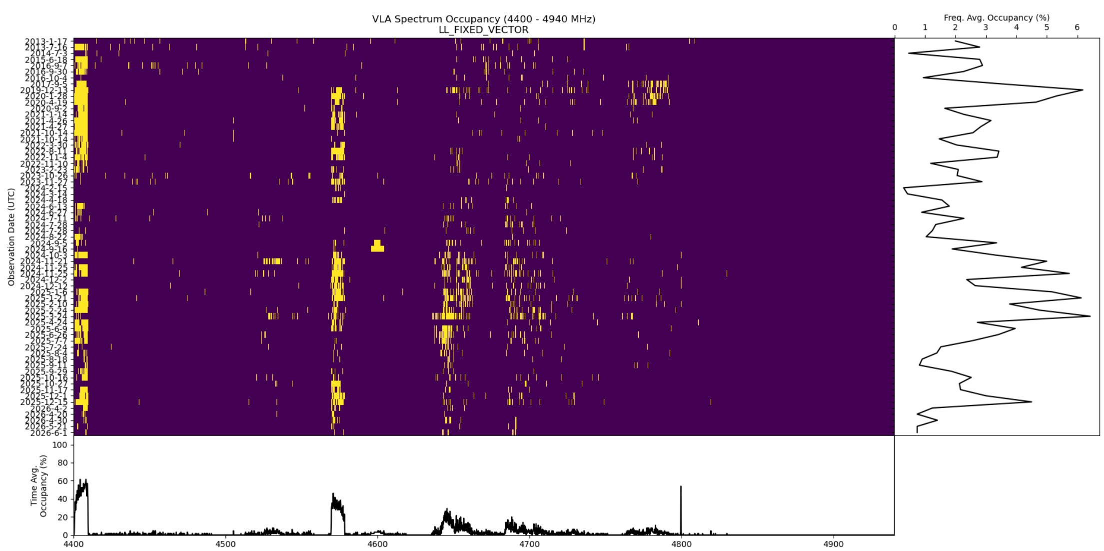

Figure 33: (Main) Waterfall plot showing spectral occupancy for the 4 400-4 940 MHz band. (Bottom) Time averaged spectral occupancy. (Right) Frequency/Band averaged spectral occupancy. Data from the LL correlation product for all fixed antenna NCP observations.

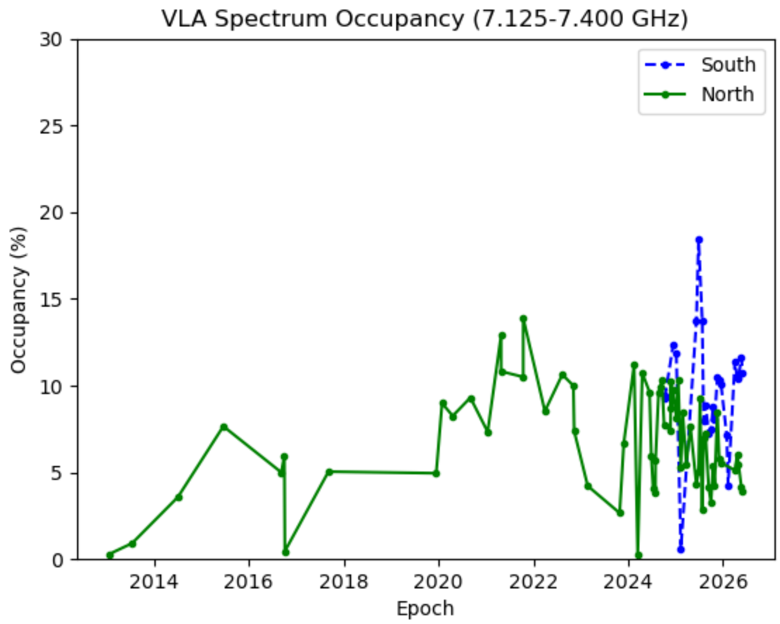

Figure 34: Study band 7 125–7 400 MHz spectral occupancy between 2013 and 2026.

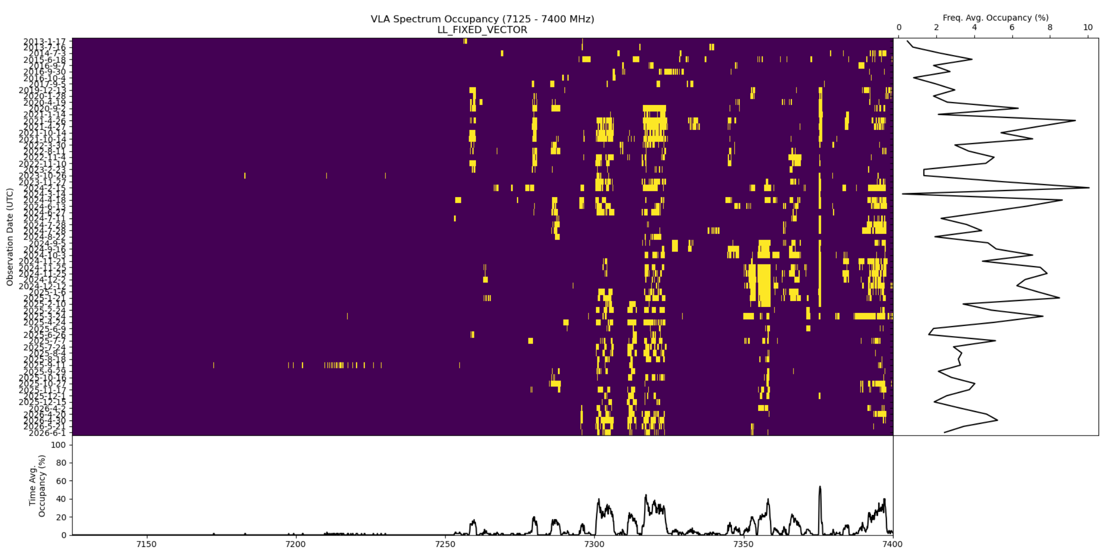

Figure 35: (Main) Waterfall plot showing spectral occupancy for the 7 125-7 400 MHz band. (Bottom) Time averaged spectral occupancy. (Right) Frequency/Band averaged spectral occupancy. Data from the LL correlation product for all fixed antenna NCP observations.

of Wifi/Bluetooth, Global Navigation Satellite Services, Mobile and select satellite communications, as well as bands that are specifically protected or administrations are strongly encouraged to protect for the use by radio astronomy.

4.4.1 Industrial, Scientific, and Medical (ISM), WiFi, Bluetooth

The industrial scientific and medical (ISM) bands are widely used by a number of applications, most commonly by WiFi, Bluetooth, and radar motion detection. As shown in Figure 36 there is a clear and dramatic rising trend for the 2 450 MHz band, as well as the 5 000 MHz one, while almost no transmissions were detected in the 24 GHz band. In Table 5 statistics is listed comparing `rfisurvey` observations from 2013-2016 with those from 2026. Zooming in on particular Wifi bands it is clear that spectral usage in the 2 450 MHz band is saturating and the trend for 5 000 MHz Wifi band usage is increasing. However, that doesn't tell the full story. In 2026, increased interference was detected at the VLA at particularly short baselines in the 5 800 MHz range. Further investigation by engineers turned up that motion detector light bulbs increasingly installed across the VLA site since 2020 were largely responsible for this rise. The light bulbs were replaced with infrared motion detections instead of radar and that interference significantly dropped subsequently, as can be seen in Figure 37 that provides a zoomed-in version for the relevant frequency range. The Wifi 6E and Wifi 7 standards make use of the 5 925–7 125 MHz band that is shared with other services, such as Microwave links, Fixed Satellite Service, and others. Thus the constant occupancy since 2013 appears to be driven by those services rather than the use of Wifi 6E/7 around the VLA.

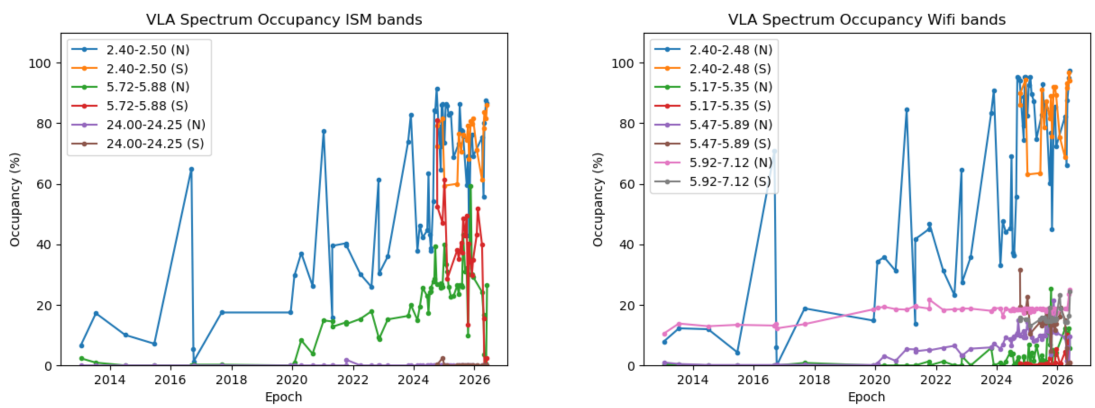

Figure 36: Left: ISM bands spectral occupancy between 2013 and 2026. Right: U.S. Wifi bands 2013–2026.

Table 5: Occupancy statistics for three ISM bands between 2013-2016 and 2026 and U.S. Wifi bands.

Range (GHz)	2013-2016 (%)	2026 N (%)	2026 S (%)	Δt (%)
2.4–2.5	8.6±4.2	80±12	80.1±8.5	71±13
5.725–5.875	0.46±0.96	17±11	16±21	16±11
24.0–24.25	0	0	0	0
2.400–2.4835	9.9±3.2	87±11	92±11	77±11
5.170–5.350	0	10.7±2.5	0.88±3.3	10.7±2.5
5.470–5.895	0	6.1±3.8	5.7±7.7	6.1±3.8
5.925–7.125	13.2±1.3	18.8±2.8	16.4±4.0	5.6±3.1

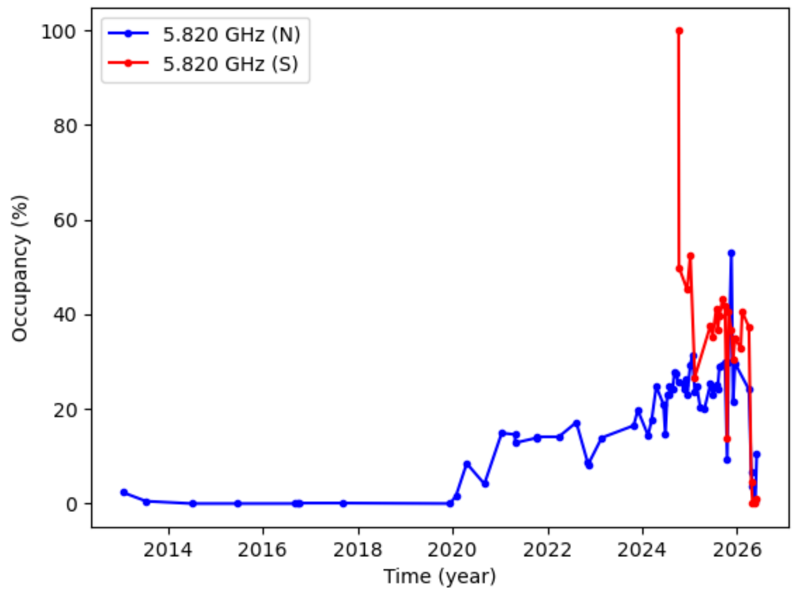

Figure 37: Recent C-band RFI caused by motion detecting light bulbs transmitting in the 5 800 GHz range. The shown occupancy is for a 128 MHz spectral window centered at 5 810 MHz.

4.4.2 International Mobile Terrestrial (IMT) above 1 000 MHz

There are a significant number of bands that are being used for IMT services up- (from cellphone to tower) and downlink (from tower to cellphone). Around the VLA there has been no notable deployment of IMT services above 1 000 MHz until 2026, when a wireless provider upgraded a nearby tower to transmit at frequencies falling into the L- and S-band receivers as noted earlier. The analysis here is to establish past and current spectral occupancy in those bands of future concern that might become occupied if other towers in the area receive technology upgrades, if no prior coordination happened. In the following discussions IMT bands are grouped by VLA receiver.

1 000–2 000 MHz

In this frequency range fall the following IMT bands:

- 1 695–1 780 MHz: AWS-1; AWS-3 Uplink
  - NCP median occupancy: 1.6±3.2%
  - South median occupancy: 7.0±8.4%
- 1 850–1 920 MHz: PCS Uplink, AWS-H
  - the NCP pointing shows no emission in this band
  - the South pointing shows a median occupancy of 2.0±3.9%
- 1 930–2 200 MHz: AWS-1; AWS-3; AWS-4 Downlink - also note first use of D2D by Starlink in 1990–1995 MHz
  - NCP median occupancy: 68±11%
  - South median occupancy: 68±13%

Figure 38 shows that most of the detected IMT emissions are due to the recent cell tower upgrade, where in a new steady state some of the IMT bands in L-band will show increase occupancy depending on time of day. Some initial transmissions were enabled for the AWS band, but subsequently were turned off for the sectors most affecting the VLA. Thus a drop in occupied spectrum can be seen in the last data points. For more information see Lawson et al. (2026). The new Starlink D2D (or DtC)[5] service is within the 1 830–2 010 MHz range, but doesn't appear to dominate spectral occupancy due to it being limited to 5 MHz within that range.

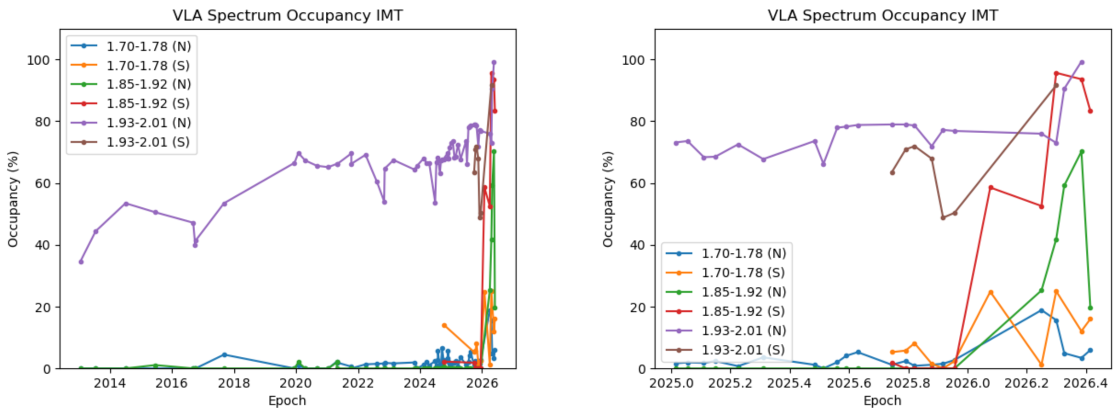

Figure 38: Left: Spectral occupancy for IMT transmission bands detected with the VLA at L-band between 2013–2026. Right: The same as on the left zoomed in to the time range of 2025–2026.5

2 000–4 000 MHz

In this frequency range fall the following IMT bands:

- 1 930–2 200 MHz: AWS-1; AWS-3; AWS-4 Downlink
  - NCP median occupancy: 40.0±8.3%
  - South median occupancy: 33±21%
- 2 300–2 400 MHz: Uplink
  - NCP median occupancy: 40.2±8.4
  - South median occupancy: 51±12
- 2 496–2 690 MHz: Broadband Radio Service/Educational Broadcast Service
  - NCP median occupancy: 11±16
  - South median occupancy: 0
- 2 570–2 620 MHz: IMT-E
  - NCP median occupancy: 2.6±16%
  - South median occupancy: 0
- 3 450–3 550 MHz: C-band
  - NCP median occupancy: 6.4±4.9%
  - South median occupancy: 19.8±4.2%

[5] DtC = Direct to Cell

- 3 550–3 700 MHz: CBRS
  - NCP median occupancy: 5.1±3.5%
  - South median occupancy: 27±11
- 3 700–3 980 MHz: C-band
  - NCP median occupancy: 72±25%
  - South median occupancy: 94.4±3.8%

Figure 39 shows for the NCP pointing and presents a relatively stable picture, where the 3 700–3 980 MHz band shows a decrease in occupancy over the past few years, likely driven due to services transitioning out of this band to make room for terrestrial wireless communications. The 1 990–2 200 and 2 500–2 690 MHz bands however show an apparent increase in spectral occupancy. Besides the recent activation of new cell tower transmissions as seen by the most recent spike in the top plot of Figure 39, it is unclear at this point what drives those emissions and requires further investigation.

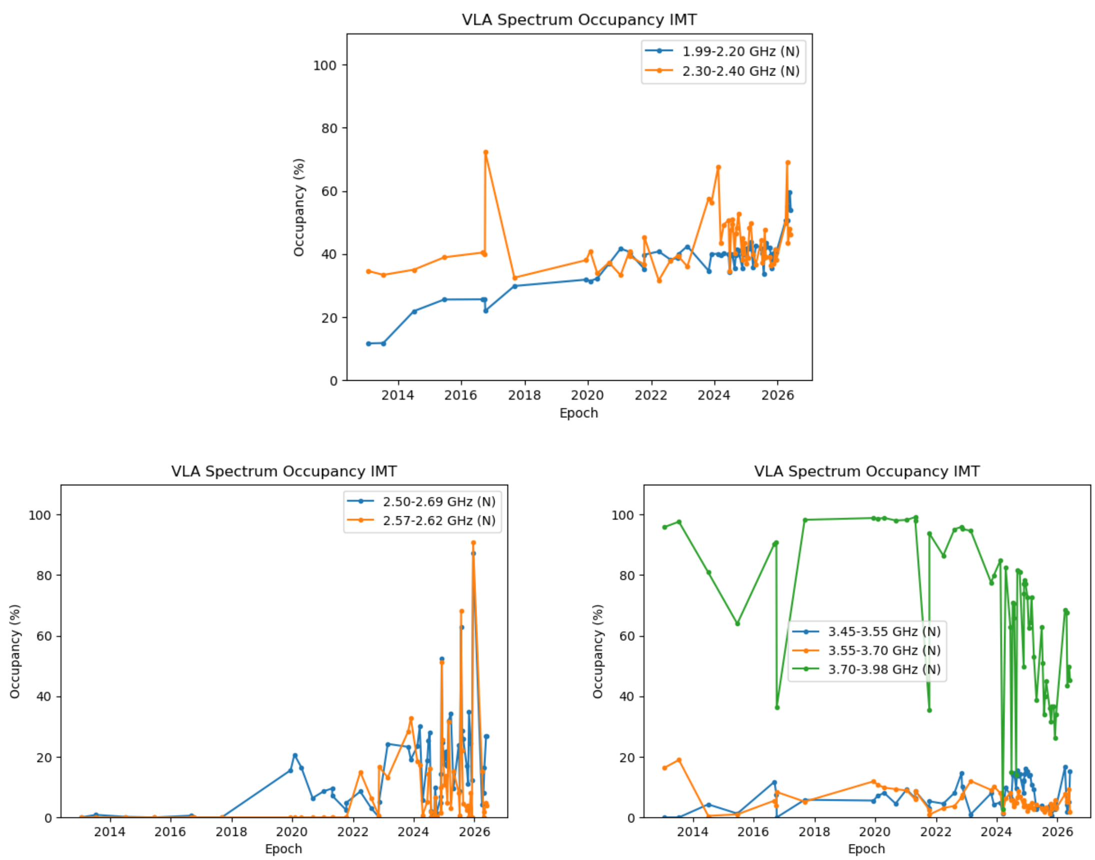

Figure 39: Spectral occupancy for IMT transmission bands detected with the VLA at L-band between 2013–2026 for the NCP pointing. The bands are separated into three different plots and only show the Northern pointing only for better clarity.

4 000–8 000 MHz

In this frequency range fall the following IMT bands:

- 5 150–5 925 MHz: U-NII-1-4

This band is in the United States available for unlicensed use primarily Wifi and short-range broadband, however also the ISM band falls within this range, as discussed above. The 5 150–5 250 MHz range is designated for low-power indoor WiFi use, the 5 250–5 725 MHz band is used for bith indoor and outdoor wireless networks using dynamic frequency selection, the 5 725–5 850 MHz range band is used for point-to-point bridging, Wifi, and Wireless Internet Service Providers, 5 850–5 895 MHz is used for unlicensed indoor operations to boost Wifi capacity, finally 5 895-5 925 MHz is designated for vehicular communications. Figure 40 shows the overall band usage in this frequency range, which appears dominated by local emissions from the motion detecting light bulbs mentioned earlier that transmit around 5 800 MHz. Thus, currently this band is mostly clear of IMT related transmissions.

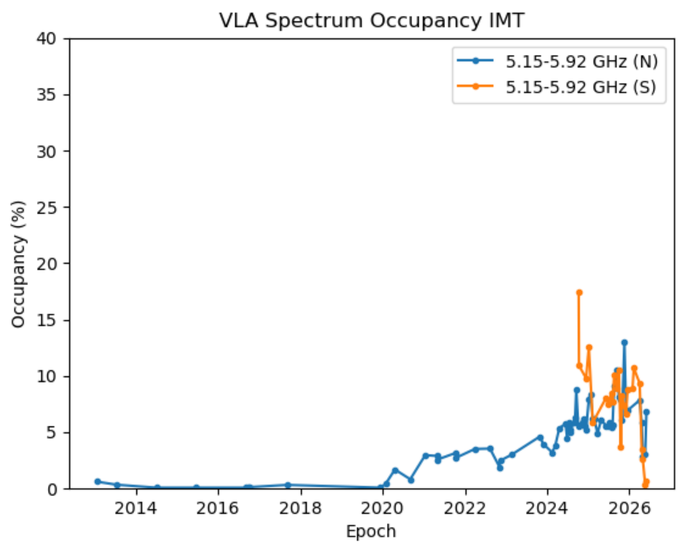

Figure 40: Left: Spectral occupancy for IMT transmission bands detected with the VLA at C-band between 2013–2026.

mmWave (24–48 GHz)

The mmWave bands 24.250–28.350, 37–40, and 47.2–48.2 GHz are not detected at the VLA, given that all frequencies above 18 GHz are virtually unoccupied in the presented survey observations.

4.4.3 Global Navigation Satellite System (GNSS)

GNSS is the general terms for satellite constellations providing positioning, navigation, and timing (PNT) services. It includes systems like GPS, Galileo, BeiDou, and GLONASS. Figure 41 shows the band plan for the major GNSS constellations. The used frequencies can be broken down into the following four blocks:

- 1 164–1 254 MHz: NCP median occupancy 85.1±7.4%
- 1 260–1 300 MHz: NCP median occupancy 91.0±3.5%
- 1 544–1 545 MHz: NCP median occupancy 100±3.0%
- 1 559–1 610 MHz: NCP median occupancy 93.3±4.1%

Given that these transmissions originate from satellite constellations that transmit to anywhere on the planet, these signals block radio astronomical observations in these bands everywhere on Earth. Figure 42 shows for the NCP pointing the temporal evolution of spectral occupancy. The plot shows that

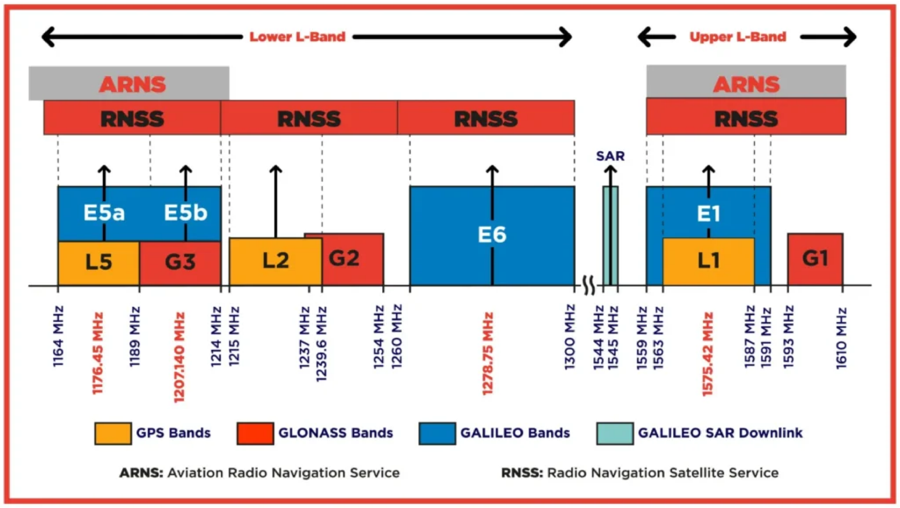

Figure 41: Band plan showing channel plan for GPS, Galileo, GLONASS, and BeiDou. The image was obtained from www.tualcom.com

spectral occupancy grew up until around 2020 and has been at a steady state since then with almost complete spectral occupancy of these bands. The above listed median occupancy values were derived for this steady state period from 2020 to 2026.5.

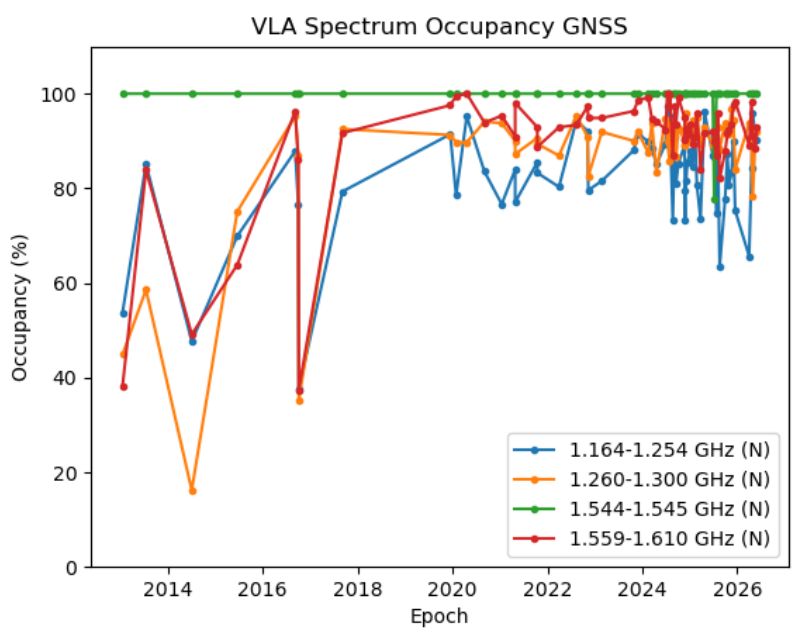

Figure 42: Spectral occupancy of the four primary GNSS bands from 2013-2026 as seen by the VLA for the NCP pointing.

4.5 Select satellite bands

Here we highlight some additional satellite bands that have been of interest. Iridium operates its User-to-Satellite communications in the 1 616–1 626.5 MHz range. For Starlink of interest is the downlink band 10.7–12.7 GHz, as well as D2D communications from 1 990–1 995 MHz. Note that for Starlink a zone of avoidance is in place that potentially attenuates the received signals by not placing downlink beams directly on the VLA. The `rfisurvey` observations currently do not invoke telescope boresight avoidance, see Nhan, De Pree, Iverson, et al. (2024), Nhan, De Pree, Beasley, et al. (2025), and Nhan, De Pree, Wasik, et al. (2026). Also note that other satellite operators use the same frequency range as Starlink, such as Eutelsat OneWeb or Amazon Leo. Planet also operates a significant satellite constellation which downlinks in the 8 025-8 400 MHz range, however given that no nearby gateways exist the VLA occupancy in that band is 0.

Iridium band usage between 2013 and 2026 has been steady at a median occupancy of 82±13%, while the Starlink DtC transmission only very recently turned on with a lot of variability while the constellations was growing up until now with universal coverage the spectral occupancy is approaching 100% for that 5 MHz band, leading to a total loss for radio astronomical observations at the VLA in this range. Figure 43 shows the temporal evolution of spectral occupancy for the discussed satellite bands.

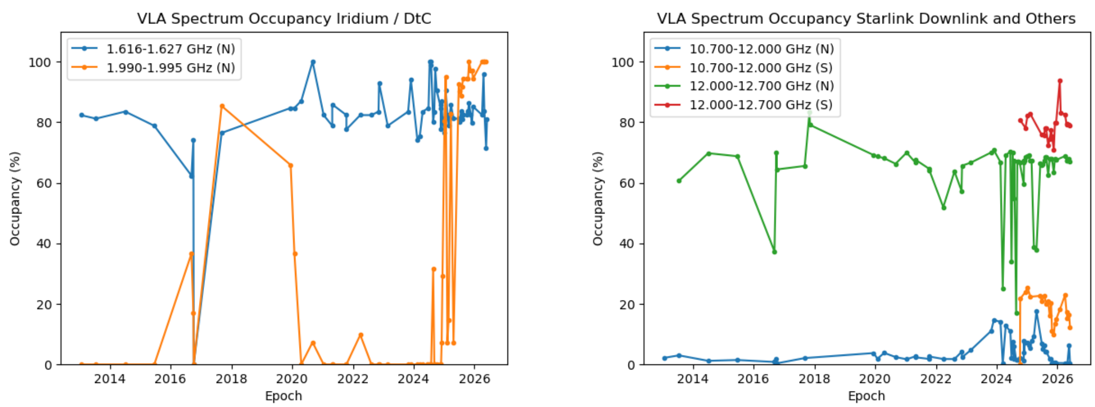

Figure 43: Left: Spectral occupancy of the NCP pointing for the Iridium and Starlink DtC band Right: Spectral occupancy of the 10.7–12.7 GHz band that includes Starlink satellite downlinks.

4.6 Radio Astronomy Bands

4.6.1 5.340 bands

All emissions is prohibited in these bands per ITU. The bands are as expected unoccupied from external signals. If the band shows some occupancy it does not necessarily mean that external emission is received, aliased signals or intermodulation products have shown to also appear in protected bands. Coincidentally the protected band at 2 690–2 700 MHz showed a strong spike in a single rfi-sweep scan in 2026 reaching up to 70%. The protected 5.340 bands are:

- 1 400–1 427 MHz
- 2 690–2 700 MHz
- 10.68–10.7 GHz
- 15.35–15.4 GHz

- 23.6–24 GHz
- 31.3–31.5 GHz
- 31.5–31.8 GHz
- 48.94–49.04 GHz

4.6.2 5.149 bands / primary RAS

All practicable steps should be taken to protect radio astronomy in these bands per ITU. These bands are:

- 322–328.6 MHz
- 406.1–410 MHz
- 1 300–1 400 MHz
- 1 610.6–1 613.8 MHz
- 1 660–1 670 MHz
- 4 990–5 000 MHz
- 10.6–10.68 GHz
- 22.1–22.5 GHz
- 22.55–23.55 GHz
- 31.5—31.8 GHz
- 42.5—43.5 GHz

Among the bands below 1 000 MHz, the 322–328.6 MHz band is unoccupied, while the 406-410 MHz band shows to be fully occupied, this is likely an artifact due to strong emissions surrounding this band, although further investigation would be warranted. The 1 300–1 400 MHz band shows a median occupancy of 9.8$\pm$2.0% for NCP. For the NCP pointing the 1 610.6–1 613.8 MHz band shows occasional excursions to higher occupancy, the South pointing is fully occupied. The 1 660–1 670 MHz band shows mostly no occupancy with the exception of some one time events. Both P and L-band have a lot of RFI signals that complicate thresholding for occupancy determination. These outliers could be a result of that. All higher frequency bands show no occupancy in the 5.149 bands between 2013 and 2026.

5 Summary and Conclusions

This memo presented an analysis of spectral occupancy at the VLA using RFI survey observations spanning 2013 to 2026, covering the P-band (230-–470 MHz) and the L- through Q-band receivers (1-–50 GHz). Occupancy was determined per receiver band, per 128 MHz spectral window (16 MHz for P-band), and for custom frequency ranges of interest, using vector-averaged cross-correlations from fixed, shortest, and longest baseline triangles with an empirically calibrated noise threshold. General findings are:

- The long-term trends show a clear degradation of the RFI environment below 8 GHz.

- Over the past decade, spectral occupancy increased by 0.77±0.11% year at L-band, 0.19±0.15% year at S-band, and 0.422±0.062% year at C-band, corresponding to a loss in usable bandwidth of approximately 145 MHz at L-band, 152 MHz at S-band, 244 MHz at C-band, and 204 MHz at X-band.
- P-band occupancy remained comparatively stable at a median of 32%. Ku-band showed no significant trend, and Ka, and Q bands remain virtually unoccupied, indicating that frequencies above 18 GHz are still largely pristine at the VLA site.

Several developments in 2026 stand out:

- The technology upgrade of a nearby cell tower introduced new IMT transmissions falling into the L- and S-band receivers, producing pronounced occupancy spikes, particularly in the Southern pointing; partial deactivation of the sectors most affecting the VLA reduced, but did not eliminate, the elevated baseline occupancy, see Lawson et al. (2026).
- Motion-detecting light bulbs installed at the VLA site itself were identified as the source of increased 5 800 GHz interference at short baselines, and their replacement with infrared-based detectors substantially reduced that contribution — demonstrating the value of combining the survey data with on-site engineering investigation for locally generated RFI.

The comparison of Northern and Southern pointing, available since 2024, shows systematically higher occupancy toward the South in most bands (e.g., ∆N-S of 7.2±4.3% at L-band and 11.7±4.0% at S-band), consistent with terrestrial transmitters and geostationary satellites entering through low-elevation sidelobes and the main beam. For a full survey of spectral occupancy one would need to sample a large range of pointings, e.g. we do not have data for East or West pointings where different terrestrial receivers might be picked up. An example for such survey is described in Schinzel (2018). Configuration-based analysis confirms that short baselines detect substantially more interference than long baselines, reflecting the spatial filtering of the interferometer; occupancy on the longest baselines in A configuration is a factor of several lower than on the shortest baselines in the compact configurations.

Regarding the NTIA study bands, the 1 680—1 695 MHz band is effectively lost to radio astronomy due to near-continuous GOES-R transmissions (85—93% occupancy), while the 2 690-–2 900 MHz and 4 400–4 940 MHz bands currently show low to no occupancy (2—3%) and the 7 125-–7 400 MHz band moderate occupancy (7—10%). The pending auction band at 3 980–4 200 MHz is already heavily occupied as seen by the C-band receiver. Should high-power commercial wireless use be introduced in the currently quiet study bands, the experience with the recent cell tower upgrade suggests significant potential impact on opportunistic observations in those ranges absent prior coordination with license owners.

GNSS transmissions continue to render the four primary navigation bands between 1 164 and 1 610 MHz almost completely occupied (median occupancies of 85—100% since 2020), and Iridium usage remains steady at 82±13%. The recently activated Starlink D2D service now approaches 100% occupancy in its 5 MHz allocation at 1 990—1 995 MHz, constituting a new total loss for observations in that range. The ITU-protected 5.340 bands remain clean of persistent external emission, and most 5.149 bands show little to no occupancy, although occasional excursions — likely intermodulation or thresholding artifacts from the RFI-rich P- and L-band environments.

Overall, these results underscore that the usable spectrum for radio astronomy at the VLA continues to erode from the bottom up, driven by satellite constellations, terrestrial wireless expansion, and locally generated interference. Continued bi-weekly RFI sweeps, the addition of the Southern pointing, and coordination with spectrum regulators and operators — as exercised in the cell tower and light bulb cases — remain essential tools for characterizing and mitigating these impacts. A future revision of this memo should fill in the missing Southern pointing D-configuration data and further investigate the unexplained occupancy increases in the 1 990-–2 200 MHz and 2 500—2 690 GHz bands.

6 Acknowledgments

The authors thank the SMD team for reviewing this memo before publication, especially Bang Nhan, Sheldon Wasik, and Chris De Pree. We also acknowledge the contributions of the NM Operations staff who enabled collection of the underlying data of this memo for more than a decade. The National Radio Astronomy Observatory (NRAO) and the Green Bank Observatory (GBO) are facilities of the National Science Foundation (NSF) operated under cooperative agreement by Associated Universities, Inc (AUI). This work is supported by the NSF's SII-NRDZ (AST-2232159) and NRAO's contribution to NTIA 7 GHz Band Study (AST-2500397).

References

Lawson, Aaron et al. (2026). *RFI Memo 168 - Impacts of New Technologies at the Gray Hill Tower on VLA Operations*. Tech. rep. National Radio Astronomy Observatory. URL: https://library.nrao.edu/public/memos/rfi/RFI_168.pdf.

Nhan, Bang D., Christopher G. De Pree, Anthony Beasley, et al. (2025). "ODS: A Self-Reporting System for Radio Telescopes to Coexist with Adaptive Satellite Constellations". In: *IEEE Communications Magazine* 63.11, pp. 146–151. DOI: 10.1109/MCOM.001.2500125.

Nhan, Bang D., Christopher G. De Pree, Matt Iverson, et al. (Aug. 2024). "Toward Spectrum Coexistence: First Demonstration of the Effectiveness of Boresight Avoidance between the NRAO Green Bank Telescope and Starlink Satellites". In: *Astrophysical Journal Letters* 971.2, L49, p. L49. DOI: 10.3847/2041-8213/ad6b24. arXiv: 2407.21675 [astro-ph.IM].

Nhan, Bang D., Christopher G. De Pree, Sheldon Wasik, et al. (2026). *Lessons learned from ongoing coordination between NRAO/GBO and LEO NGSO satellite constellations*. arXiv: 2607.08875 [astro-ph.IM]. URL: https://arxiv.org/abs/2607.08875.

Perley, Rick (2002). *EVLA Memo 49 - Attenuation of Radio Frequency Interference by Interferometric Fringe Rotation*. Tech. rep. National Radio Astronomy Observatory. URL: https://library.nrao.edu/public/memos/evla/EVLAM_49.pdf.

Schinzel, Frank (2018). *EVLA Memo 206 - S-band Radio Frequency Interference from Geostationary Satellites*. Tech. rep. National Radio Astronomy Observatory. URL: https://library.nrao.edu/public/memos/evla/EVLAM_206.pdf.